NATIONAL AERONAUTICS AND SPACE ADMINISTRATION, WASHINGTON D.C. 20546

DOE/NASA/0129-1
NASA CR-165491

DO NOT DESTROY
RETURN TO LIBRARY

Design and Evaluation of Low-Cost Stainless Steel—Fiberglass-Foam Blades for Large Wind Driven Generating Systems

Walter S. Eggert, Jr.
The Budd Company

October 1982

21 MAR 1983
MCDONNELL
RESEARCH & ENGINEERING LIBRARY
ST. LOUIS

Prepared for
NATIONAL AERONAUTICS AND SPACE ADMINISTRATION
Lewis Research Center
Under Contract DEN 3-129

for
U.S. DEPARTMENT OF ENERGY
Conservation and Renewable Energy
Wind Energy Technology Division

LM128403E

M83-12087

NOTICE

This report was prepared to document work sponsored by the United States Government. Neither the United States nor its agent, the United States Department of Energy, nor any Federal employees, nor any of their contractors, subcontractors or their employees, makes any warranty, express or implied, or assumes any legal liability or responsibility for the accuracy, completeness, or usefulness of any information, apparatus, product or process disclosed, or represents that its use would not infringe privately owned rights

DOE/NASA/0129-1
NASA CR-165491

Design and Evaluation of Low-Cost Stainless Steel—Fiberglass-Foam Blades for Large Wind Driven Generating Systems

Walter S. Eggert, Jr.
The Budd Company
Fort Washington, Pennsylvania 19034

October 1982

Prepared for
National Aeronautics and Space Administration
Lewis Research Center
Cleveland, Ohio 44135
Under Contract DEN 3-129

for
U.S. DEPARTMENT OF ENERGY
Wind Energy Technology Division
Washington, D.C. 20545
Under Interagency Agreement DE-AI01-79ET20320

TABLE OF CONTENTS

	PAGE
SUMMARY	1
INTRODUCTION	2
DESIGN REQUIREMENTS	3
BUDD DESIGN CONCEPT	10
DISCUSSION	18
PRELIMINARY DESIGN REVIEW	21
FINAL DESIGN PROGRAM	23
TEST PROGRAM	23
STRUCTURAL ANALYSIS	32
COST AND WEIGHT ANALYSIS	38
SHIPPING AND HANDLING	45
FABRICATION OF SPAR TEST ELEMENT	47
CONCLUSIONS	53

SUMMARY

This report describes the development of a low cost wind turbine blade design based on a stainless steel/fiberglass foam design concept and to evaluate its principle characteristics, its low cost features, and its advantages and disadvantages. A blade structure was designed and construction methods and materials were selected. Complete blade tooling concepts, various technical and economic analysis, and evaluations of the blade design were performed. A study was made to determine the applicability of the blade design concept to various blade lengths in the range of 15 ft. to 200 ft. A test specimen of the spar assembly, including the root end attachment, was fabricated. This 20 ft. long full-scale section will be fatigue tested by NASA.

It was concluded that the stainless steel/fiberglass-foam blade concept is a viable design for application to large wind turbine systems. A blade design was completed which meets the requirements for operation on the MOD-OA wind turbine. The design concept is applicable to various length blades. Blades less than 60 feet would use a stainless steel spar and blades of larger size would have a fusion welded carbon steel spar. The design permits a choice of a wide selectivity of air-foil shapes and, because of its modular construction, the design provides producibility and quality in high volume production.

INTRODUCTION

Studies conducted by The Budd Company Technical Center resulted in a blade concept that NASA-Lewis Research Center felt, held promise for a practical low cost wind turbine blade.

As a result of the Federal Government efforts to encourage development of alternate energy generating systems, the NASA-Lewis Research Center, acting for D.O.E., awarded contract DEN-3-129 to The Budd Company Technical Center. The contract specified the requirements for designing and evaluating a low cost blade for large wind driven generating systems.

The blade is composed of three structural elements:

A main box spar with root connection manufactured from stainless or carbon steel, leading and trailing edge modules of fiberglass reinforced plastic fabricated from low cost commercial grade material, stiffened by rigid urethane foam, and a fiberglass tip extension similar to the construction used on the leading and trailing edge modules. The fiberglass elements provide the aerodynamic surfaces.

This report covers the development of the blade design.

The purpose of the work performed under this contract is to demonstrate that the blade design meets the contract low cost objectives and the performance specifications.

DESIGN REQUIREMENTS

To provide understanding of the basic design requirements, a condensed version of the NASA-Lewis contracted specifications as well as modifications are presented as follows:

A. Blade Geometry

1. The blades shall be designed using the Airfoil Configuration NASA-230XX.

2. The blade shall have a linear twist of ten degrees from the blade root (32" from rotor center) to tip.

3. The maximum thickness of the airfoil section shall be 40% of the chord at the root and 18% of the chord at the tip and shall vary linearly between these stations.

4. The hub-to-blade flange shall be at 31.75 inch blade station. The flange at this location shall be such that the blade is capable of interfacing with the hub spindle on the Mod-OA wind turbine.

5. Acceptable blade planforms are shown in Figure 1. This figure shows a root cut-out of 25%. This is the maximum allowable cut-out and the contractor shall determine the cut-out for his design since it is desirable for performance to minimize root cut-out. Figure 2 shows the effect of root cut-out on yearly energy capture. In terms of cost tradeoff, one megawatt hour is worth approximately $100 of blade cost.

6. The blade length shall be 60 feet from hub flange to blade tip.

7. The objective of the proposed blade design shall be to minimize blade cost while achieving adequate performance. To achieve this, the following goals should be considered consistent with other requirements and manufacturing practicality:

a. Minimize the thickness-to-chord ratio

b. Minimize the solidity ratio of the blades. (Where solidity is the area of the blades divided by the area of the circle swept by the rotor).

B. Operational Considerations

1. The blade shall be designed as part of a two-bladed rotor.

2. The blade shall be designed to operate at ambient temperatures $-30^{\circ}F$ to $120^{\circ}F$ ($-35^{\circ}C$ to $49^{\circ}C$).

3. The blade shall not be susceptible to damage by sunlight, high humidity, salt spray or fungus.

C. Blade Design Loads

1. The Contractor shall design the blade to withstand the following two independent load conditions:

   a. A maximum flat wise wind load of 50 pounds per square foot on planform area.

   b. Fatigue bending moment distributions, both flatwise and edgewise, as shown in Figures 3 and 4. The cyclic edgewise load distribution shown in Figure 3 shall be scaled by the ratio of the proposed blade weight to a blade weight of 2350 pounds (i.e., if the proposed blade weight is 3525 pounds, the cyclic edgewise moment specification shall be 1.5 that shown in Figure 3).

2. Under these load conditions there shall be:

   a. No yielding of any structure under maximum wind load.

   b. No buckling of primary structure under maximum wind load.

   c. No failure in 4×10^8 cycles (30 years) under flatwise or edgewise fatigue loads. (Flatwise and edgewise positive directions are shown in Figure 5).

3. The fundamental first bending mode cantilever natural frequency (static) of the blade in the flatwise and edgewise directions shall fall in one of the following ranges:

$$1.50 \text{ Hz} \leq \omega \leq 1.85 \text{ Hz}$$

$$2.15 \text{ Hz} \leq \omega \leq 2.55 \text{ Hz}$$

$$2.75 \text{ Hz} \leq \omega \leq 3.15 \text{ Hz}$$

$$3.45 \text{ Hz} \leq \omega \leq 3.85 \text{ Hz}$$

Where ω = blade natural frequency

Note: It is permissable for the flatwise and edgewise natural frequencies to be the same.

4. Figure 6 shows an envelope of blade weight and cost. (The blade costs are those estimated as the average cost of 100 blades manufactured in one year). For a blade to be acceptable, it must fall within this envelope. Blade costs are to include all elements such as profit and amortization of tooling and engineering but shall be based on 1978 dollars (inflation shall not be considered). All blade weights are to include the weight of any flange adapter, if required. The lower cost-weight factor for a given design, the more attractive that design is.

5. The tolerance on blade weight for blade-to-blade uniformity is $\pm$ 2%. Spanwise center-of-gravity shall be on, or in front of, the 32% chordline and blade-to-blade variation of $\pm$ 1% of the chord length will be permissable.

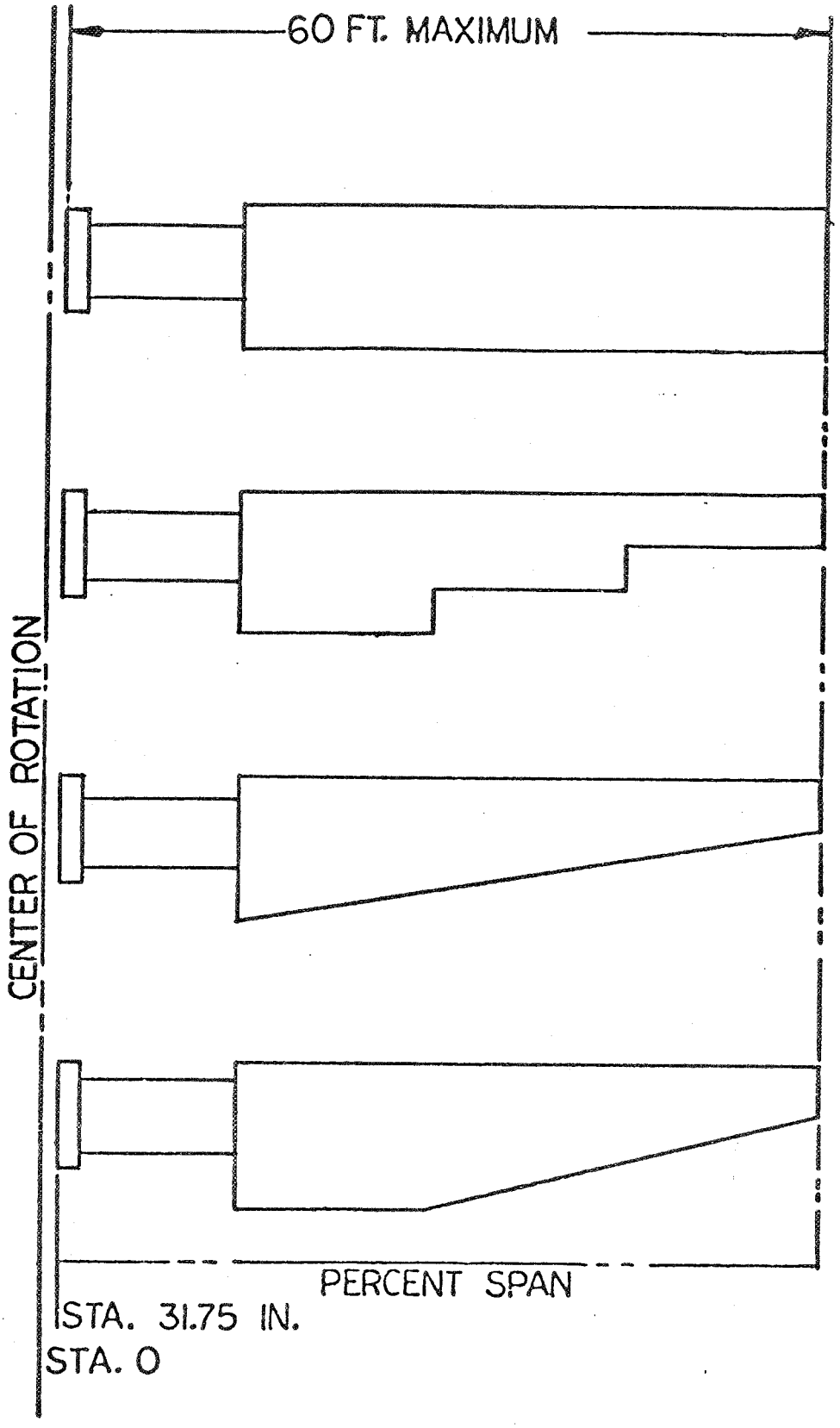

FIGURE 1 - ACCEPTABLE BLADE PLANFORMS

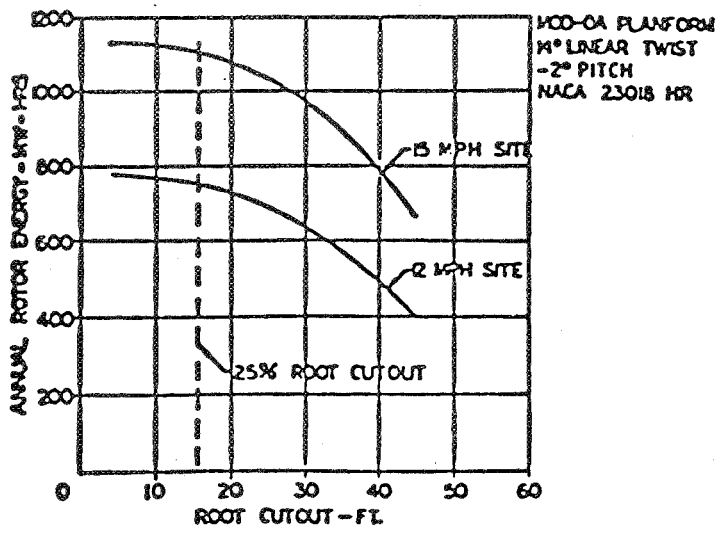

FIGURE 2 - EFFECT OF ROOT CUTOUT ON ANNUAL ENERGY

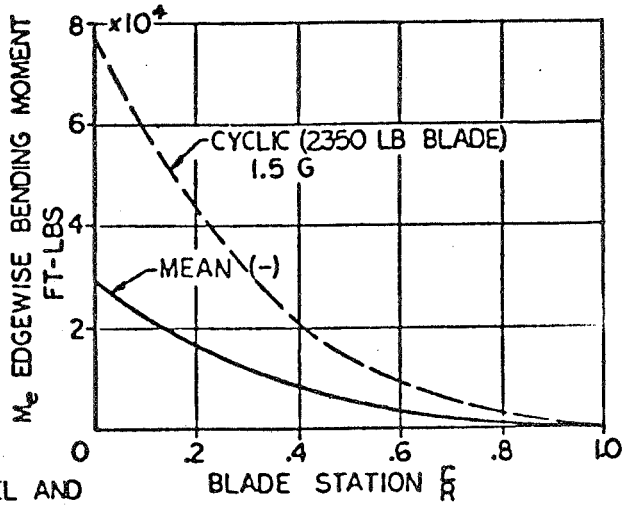

NOTE: THE MOMENT VECTORS ARE PARALLEL AND PERPENDICULAR TO THE .75 CHORD LINE

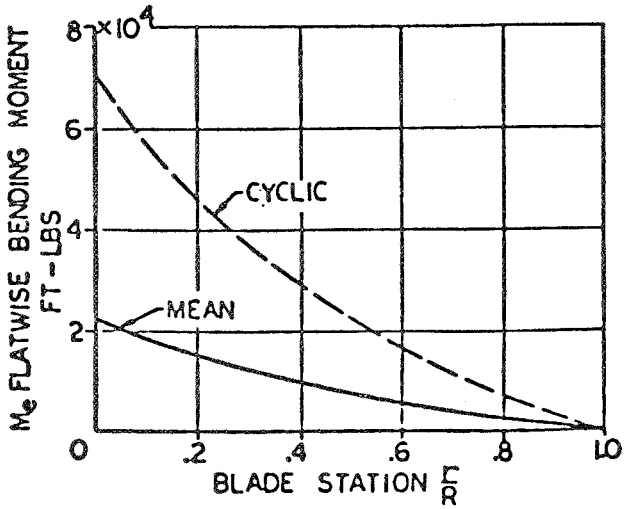

FIGURE 3 - FLATWISE & EDGEWISE BENDING MOMENT DISTRIBUTIONS

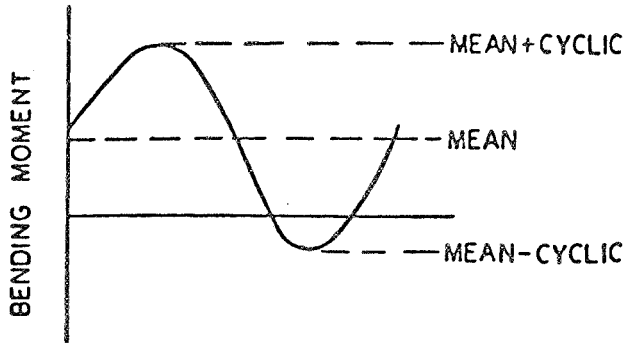

FIGURE 4 - DEFINITION OF MEAN AND CYCLIC MOMENTS

$+M_f$ - COMPRESSION IN HIGH PRESSURE SIDE

$+M_e$ - COMPRESSION IN LEADING EDGE

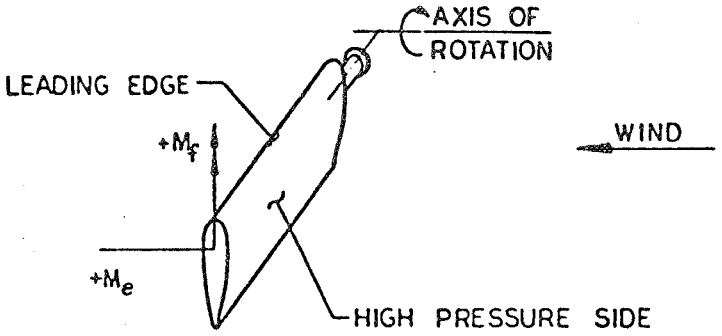

FIGURE 5 - BENDING MOMENT SIGNS CONVENTIONS

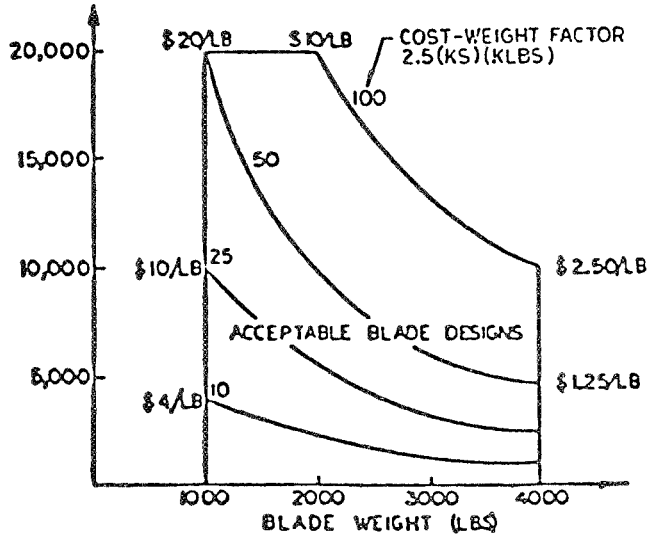

FIGURE 6 - BLADE WEIGHT VERSUS BLADE COST

D. Supplementary Design Requirements

Clarification of blade design requirements was discussed during the contract initiation meeting held at The Budd Company in Fort Washington, PA. The Government clarified that a 47,000 ft.-lb. maximum static bending moment and a 3,000 lb. max blade weight would be required to provide compatibility with the MOD-OA wind turbine operational requirements.

BLADE DESIGN

In certain designs, the leading edge section, or the D spar area of the blade, is used to carry the operating loads, and the trailing edge is essentially non-structural, carrying air loads for the trailing edge only. The Budd design does not have a conventional forward D spar. The design uses a central spine spar located within the envelope of the aerodynamic contours. This spar carries all the edgewise and flatwise loading and provides all the torsional stiffness for the blade system.

The leading edge and trailing edge fiberglass components are designed to distribute the air loads directly to the spar and are segmented span-wise to prevent them from carrying spanwise bending loads due to the spar deflections. These sections are bonded to the spar using an elastomeric adhesive. Figure 7 shows an idealized cross-section of the blade.

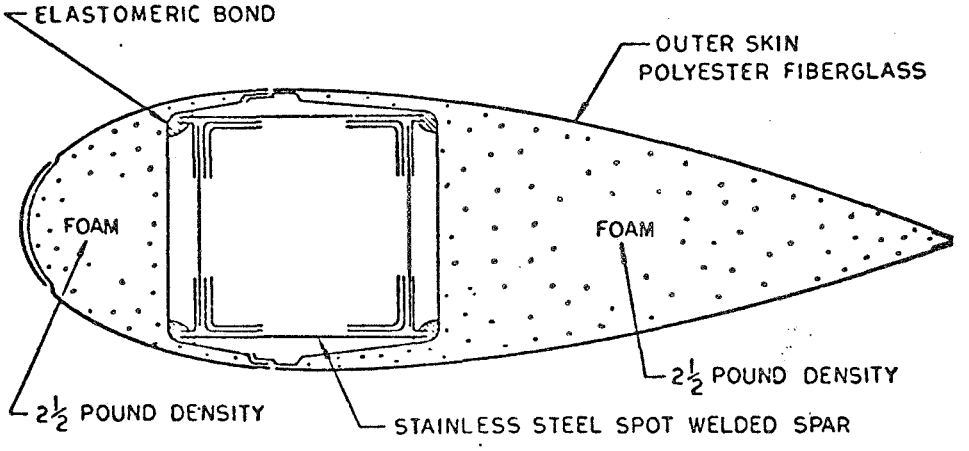

FIGURE 7 - TYPICAL SECTION WIND TURBINE BLADE

There is a center spar composed of spot welded stainless steel. This structure is composed of top and bottom cap strips, two shear webs, one on the front and one on the aft side of the spar. The spar is built with a 10^{o} twist from the root end to the outer end. The leading edge and the trailing edge assemblies are fabricated of fiberglass reinforced plastic composed of multiple pieces bonded together that are then filled with urethane foam. These fiberglass

subassemblies are bonded to the spar at the four flange corners of the spar. The leading and trailing edge assemblies are also bonded and mechanically fastened to each other at the high camber point of the blade. The leading edge of the blade is protected by an elastomeric cover sheet to provide protection against impact of hail and other abrasive elements. The leading and trailing elements are designed so as not to contribute significantly to the structural stiffness of the blade.

Shown in Figure 8 is an exploded view of the spar assembly. The spar is composed of four sub-assemblies, an upper and lower cap strip plate assemblies and front and rear spar webassemblies. The selection of stainless steel and the spot weld process provides a unique method by which the spar stiffness can be tapered effectively to provide a near uniform stress from the root end to the tip of the spar. This tapering is accomplished by the use of tapered angles that are spot welded together and are joined to the upper and lower cap strip plates. The thickness of the top plates are tapered in three steps using a butt arc weld to join each thickness. This is a specialized process that was developed during the Budd 301 testing program which is discussed in the section on the Test Program. This provides a weld of high reliability in fatigue strength. By controlling this taper, we are able to provide uniform tapering of the basic properties of the spar section. The angles are first tapered in the blank and, as a result, there is essentially no material lost. The angles are then formed and then spot welded to the spar cap assembly. This is all done in the flat and then they are elastically twisted to match the 10° twist of the spar. The spar webs are composed of two angles and spar web. The two angles and web are spot welded in place to form the web for the spar. There are two of these subassemblies which are also built flat and elastically twisted to form the 10° twist to the spar. The four subassemblies are then inserted into an assembly fixture which provides the 10° twist, and are then spot welded together. This provides a very efficient tapering of the spar without machining and at a very low cost using rolled sheet material. The use of stainless steel also provides excellent corrosion protection for long life of the spar. Spot welding is a low cost, reliable, efficient attachment process to assemble the spar.

Figure 9 shows a breakout of all the major subassemblies of the blade.

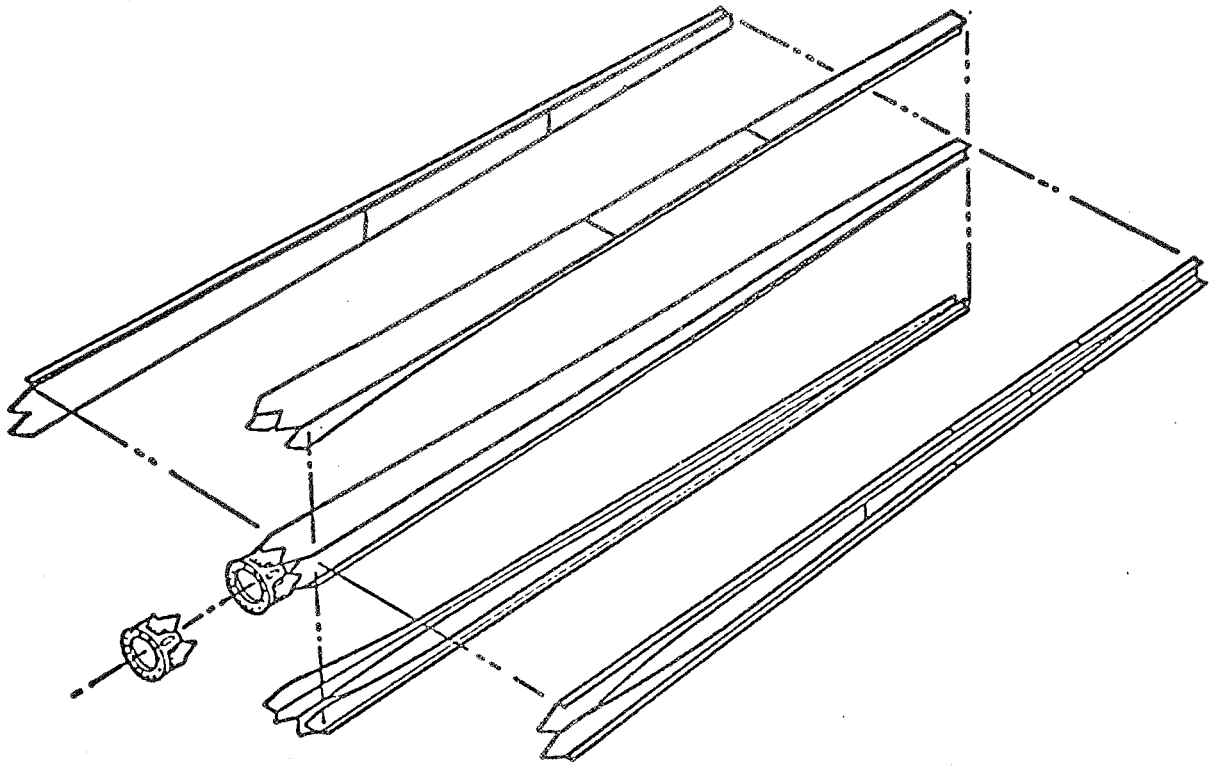

FIGURE 8 - EXPLODED SPAR ASSEMBLY

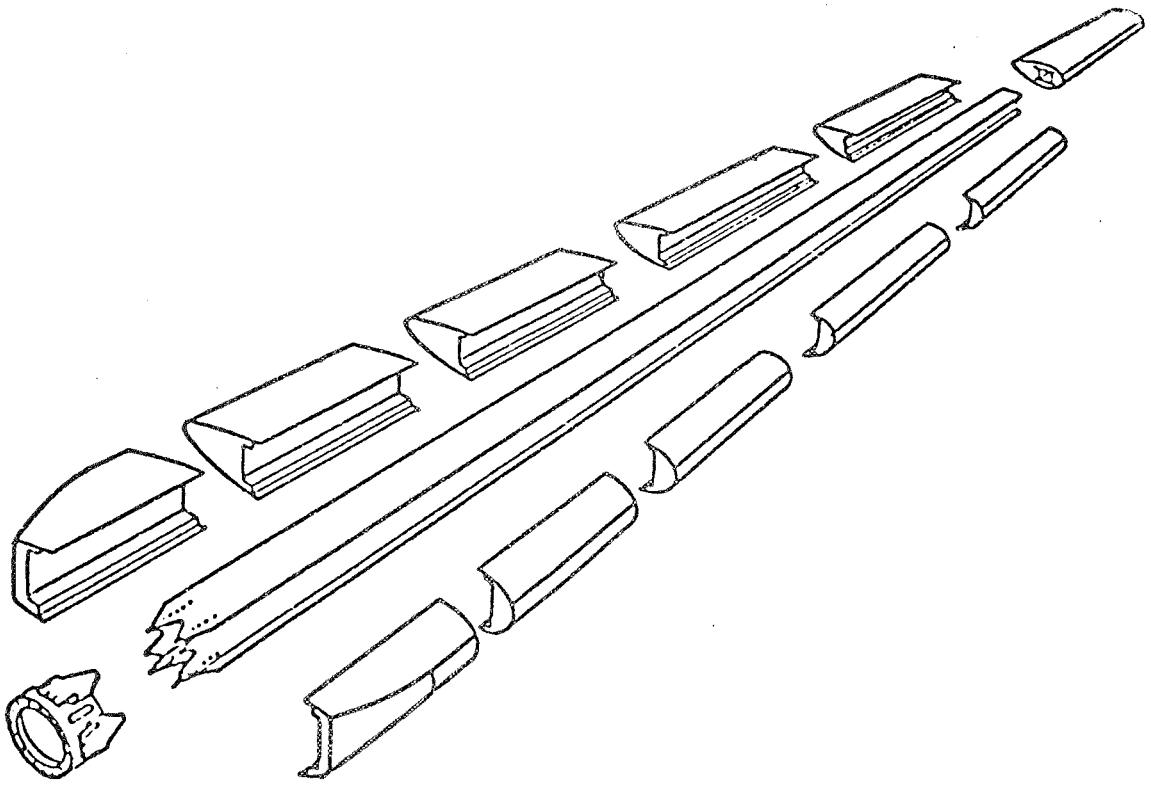

FIGURE 9 - MAJOR SUB-ASSEMBLY

Figure 10 shows an exploded view of the leading edge and trailing edge assemblies. These assemblies are composed of low cost layup of fiberglass-reinforced polyester. Fiberglass elements are parasitic to the primary spar structure and are used only to distribute the air loads to the spar. Their design requirements are minimal. To stabilize these elements for fatigue, the fiberglass elements are filled with a semi-rigid, urethane foam of approximately 2-1/2 pounds per cubic foot density. This provides a lightweight, well-damped structure for the leading and trailing edge assemblies and prevents aerodynamic flutter of the lightweight surfaces. This design permits accurate dimensional control of the aerodynamic surfaces at low cost.

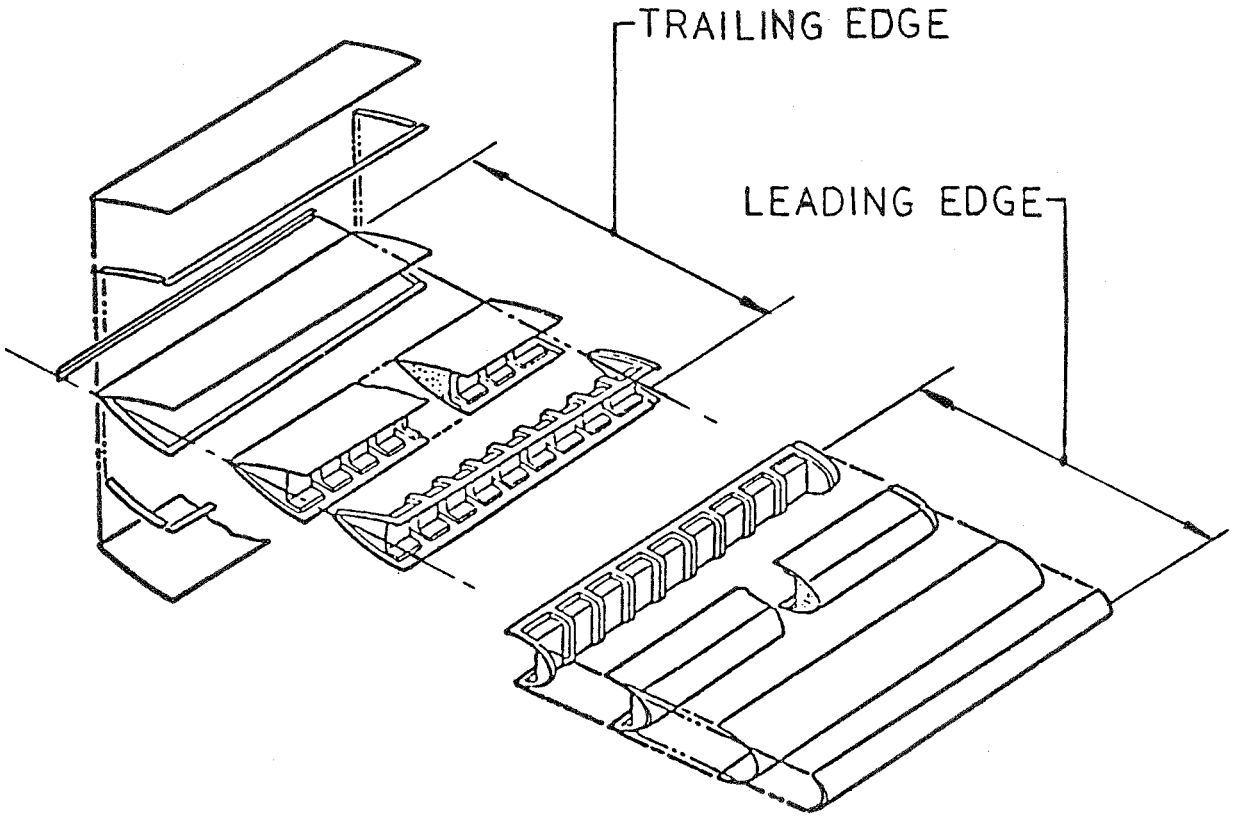

FIGURE 10 - EXPLODED VIEW OF LEADING AND TRAILING EDGE ASSEMBLIES

To reduce weight and to improve mass distribution in the blade, the metal spar is cut short and a structural fiberglass tip extension is used. Figure 11 shows a breakout view of the tip parts.

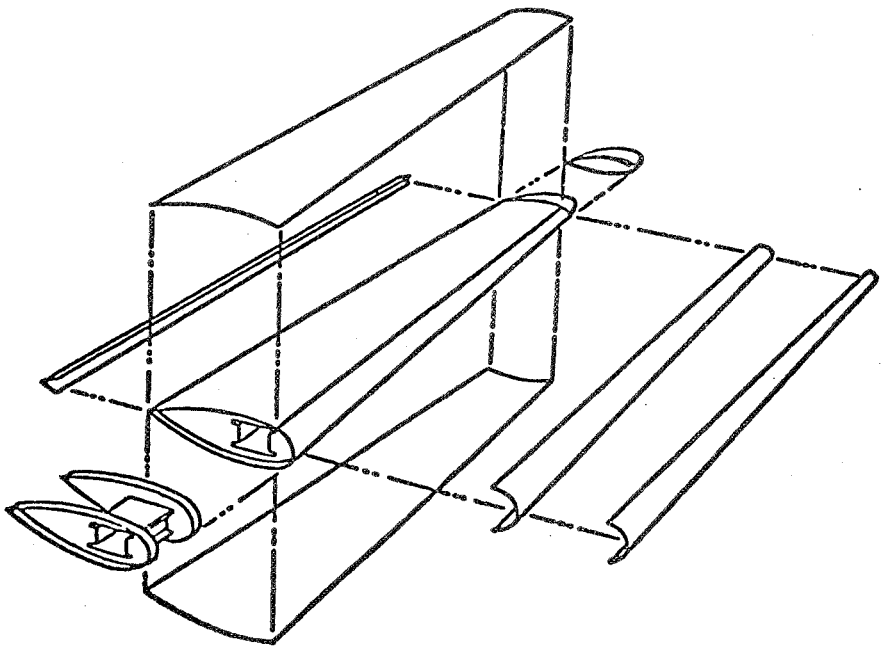

FIGURE 11 - BREAKOUT VIEW OF TIP PARTS

The final assembly of the blade is accomplished in two major steps, as shown in Figure 12. The trailing edge assemblies are bonded to the spar. Progressing from the inboard end of the blade outward, the leading edge subassemblies are then attached to the spar trailing edge major assembly by bonding and mechanical fastening. The tip assembly is then bonded and mechanically joined to the blade assembly. The final step is the installation of elastomeric sealing strips between the edges of the fiberglass assemblies to provide aerodynamic sealing of the surfaces.

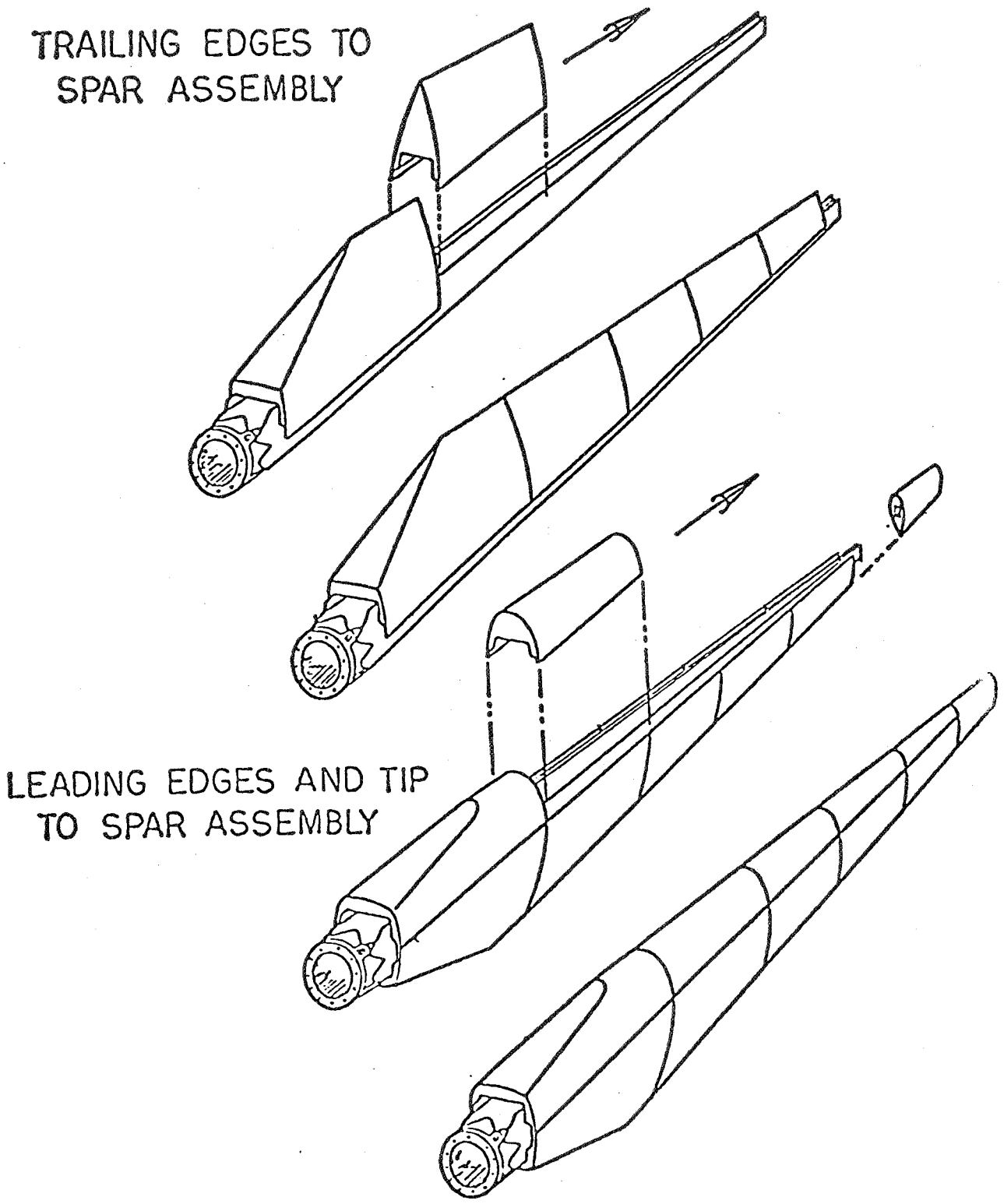

FIGURE 12 - TRAILING EDGES, LEADING EDGES AND TIP TO SPAR ASSEMBLIES

A study was performed to determine whether the basic concept of the blade design could be utilized through the entire range of blade sizes. The concept of a rectangular spar inside the aerodynamic surface carrying the principal loads with parasitic aerodynamic elements directing the air loads to the spar is applied to the entire range of blades. Figure 13 shows the blades that were included in this study. Using the present configuration with a high aspect ratio blade, the design would use stainless steel for the spar from the 60-foot size blade down to the smaller sizes. The advantage of the stainless steel spar is the ability to taper and spot weld the assemblies together at low cost and with good corrosion resistance for the thinner gage materials needed on the smaller blades. For lengths greater than 60-foot, the design would use high strength, low alloy carbon steel for the spar. The reason for this is that the gage of the materials will be beyond the range of those producible in cold-rolled stainless steels. Thicker gage cryogenic stainless steel material might be used, but we do not think this would be economically feasible in the larger size.

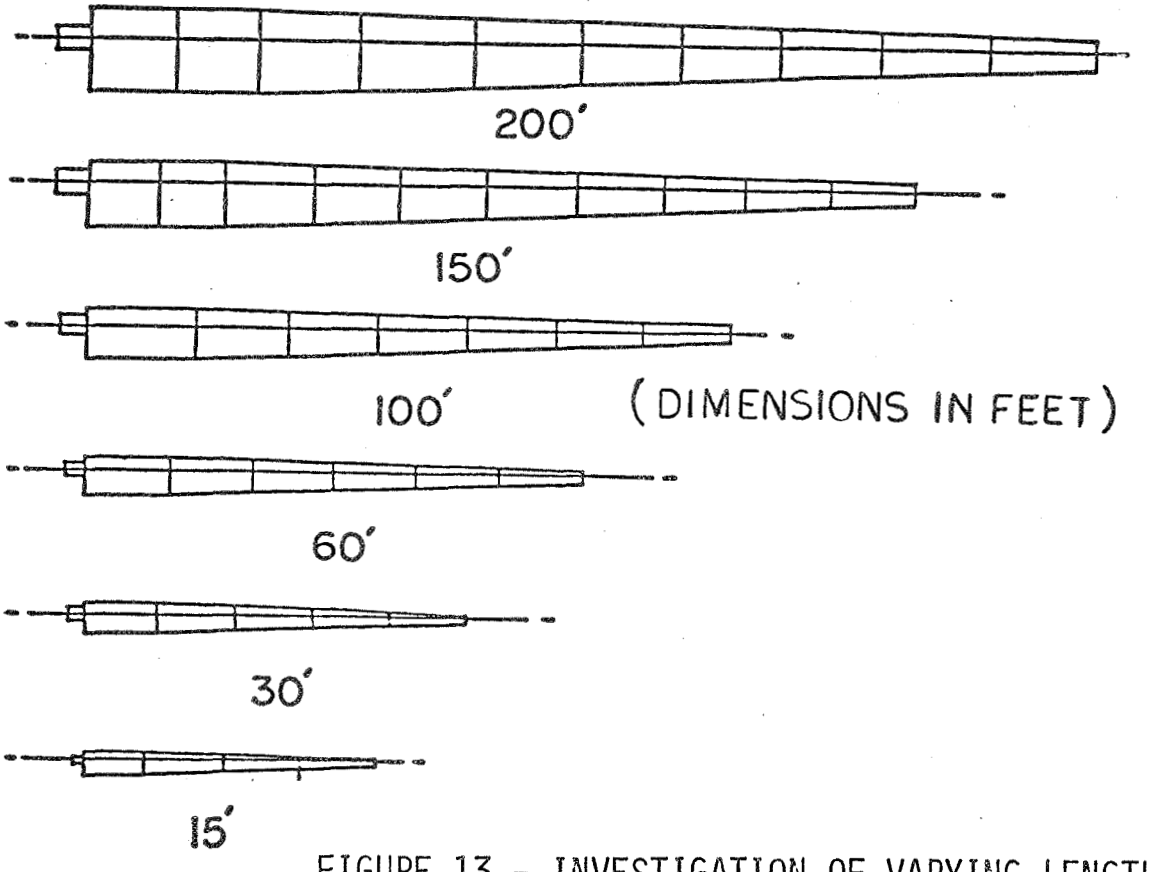

FIGURE 13 - INVESTIGATION OF VARYING LENGTHS

Figure 14 shows the spar configuration for the 60-foot blade. This is constructed of 301 1/4 hard .125 thick stainless steel. Also shown is the configuration of a spar of 200 ft. length.

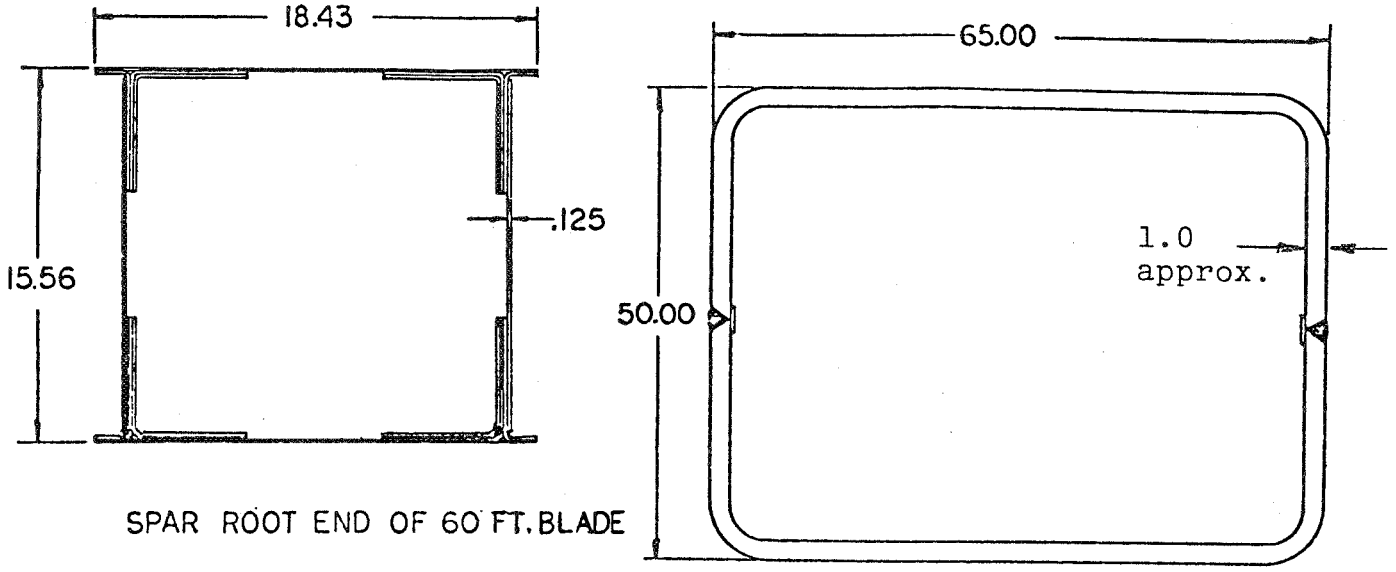

FIGURE 14 - SPAR ROOT END OF 60 FT. AND 200 FT. BLADE

Considering only production costs, it is less costly to produce a multiplicity of smaller blades rather than a low quantity of larger blades for the same power output. Since the blade is only a part of the total system, this conclusion may not hold when considering the whole system cost.

Larger blades require manufacturing activities that are beyond the present state of the art in many areas. To provide a good, low cost design will require further investigation. For transportation, a blade up to 85 feet in length can be shipped in one piece without major difficulty. Greater length blades probably would have to be shipped in multiple pieces. This, of course, increases the problems of design of the blade, as this would require spar joints outboard in the blade that require the same degree of reliability as the root fitting. This could add considerably to the weight and cost.

DISCUSSION

The design of large wind turbine blades have conflicting requirements and criteria. Cost is the most sensitive requirement and structural reliability is the foremost criterion. The Budd design is predicated on the premise that large blades should be an industrial product of predictable performance and uncomplicated structure. In order to be successful, rotors must be capable of being produced in volume at reasonable cost. The Budd Company has extensive experience in the design and manufacture of structures made of carbon steel, stainless steel, and glass reinforced plastic. Fabricating techniques combined with a long history of successful product designs provided the key to meeting the program objectives.

To achieve a potential 30 year life, the selection and evaluation of materials used is critical. It became evident early in the program that design criteria for aircraft wings and helicopter blades did not apply for a horizontal axis system. Because of the cyclical loading in the edgewise direction, the system is more analogous to a rotating fatigue machine. With a rotational speed of 40 rpm the spar structure will experience about 400 million load cycles during the life of the blade. Existing fatigue data for most materials are generally limited to the range of 2 to 10 million cycles. It is prohibitively costly and time consuming to run fatigue tests to 400 million cycles. Even at high testing rates it would take many years to obtain actual test data on full scale test elements; therefore, it was necessary to develop high cycle endurance strength by a more practical approach. To accomplish this we chose to establish the S/N curve, on the basis of test data, in the range of zero to ten million cycles-to-failure. These S/N curves were then extrapolated graphically to four hundred million cycles-to-failure. To determine the fatigue strength for a different R value (i.e., ratio of minimum to maximum stress) the modified Goodman Diagram was used. This technique was applied for both parent material and splices--e.g., spot welded or butt fusion welded connections. The above described procedures have their principle application to base material properties. When applying this technique to welded configurations and complete systems, there can be some risk associated with the selected stress values. Complete systems have to be tested to provide final proof of the design. Therefore, a full scale section of the spar, including the root end, was fabricated and delivered to NASA-Lewis Research Center for testing.

To supplement the full scale test elements, The Budd Company using it's own funds, conducted an independent test program to obtain long term fatigue data for 301 1/4 hard material,

including fusion welding as well as spot welding. The results of this activity were used to provide additional data for the blade program.

The fiberglass leading and trailing edge assemblies that form the aerodynamic surfaces were tested as a complete system, by fabricating a one foot wide section representative of Sta. 187 inches on the blade. The maximum aerodynamic load was simulated by bonding masses to the outer surface of the test element which then was cycled on a shaker test fixture at resonance of the specimen.

Summary data from these test programs are presented in the section on the final design program.

One of the principle outputs required of the contract was to confirm the low cost aspects of the Budd design. To accomplish this, a weight and cost analysis was conducted. The blade final design was processed in detail and manufacturing and tooling costs were determined. This was done for quantities of 2, 10, 100, and 1000 per year. The design was reviewed over the range from 15 ft. to 200 ft. blade size and the blade design proved to be practical. The design study indicated that various spar materials should be used depending on the practicality of application relative to blade size. The detail costing was centered on the Mod. O.A. blade of 60 ft. size. The estimated cost summary for 100 blades per year is shown on Figure 15, and as can be seen in the chart from the NASA specification, the Budd blade falls well within the cost objectives set out by the contract.

The final design presented at NASA-Lewis Research Center, was accepted subject to final test results of the test spar section.

ESTIMATED COST SUMMARY
BASED ON 100 BLADES ANNUALLY

TOOL COST

Tools 1,215,000

Based on Production of 100 Blades Annually

Tool Cost 1,215 Per Blade

(Tools Prorated on 10 Years Production)

COST SUMMARY

Material	4,600
Labor	5,570
Tools	1,215
Total	11,385
5% G&A	570
Total Cost	11,955
10% Profit	1,195
Cost & Profit	13,150 Per Blade

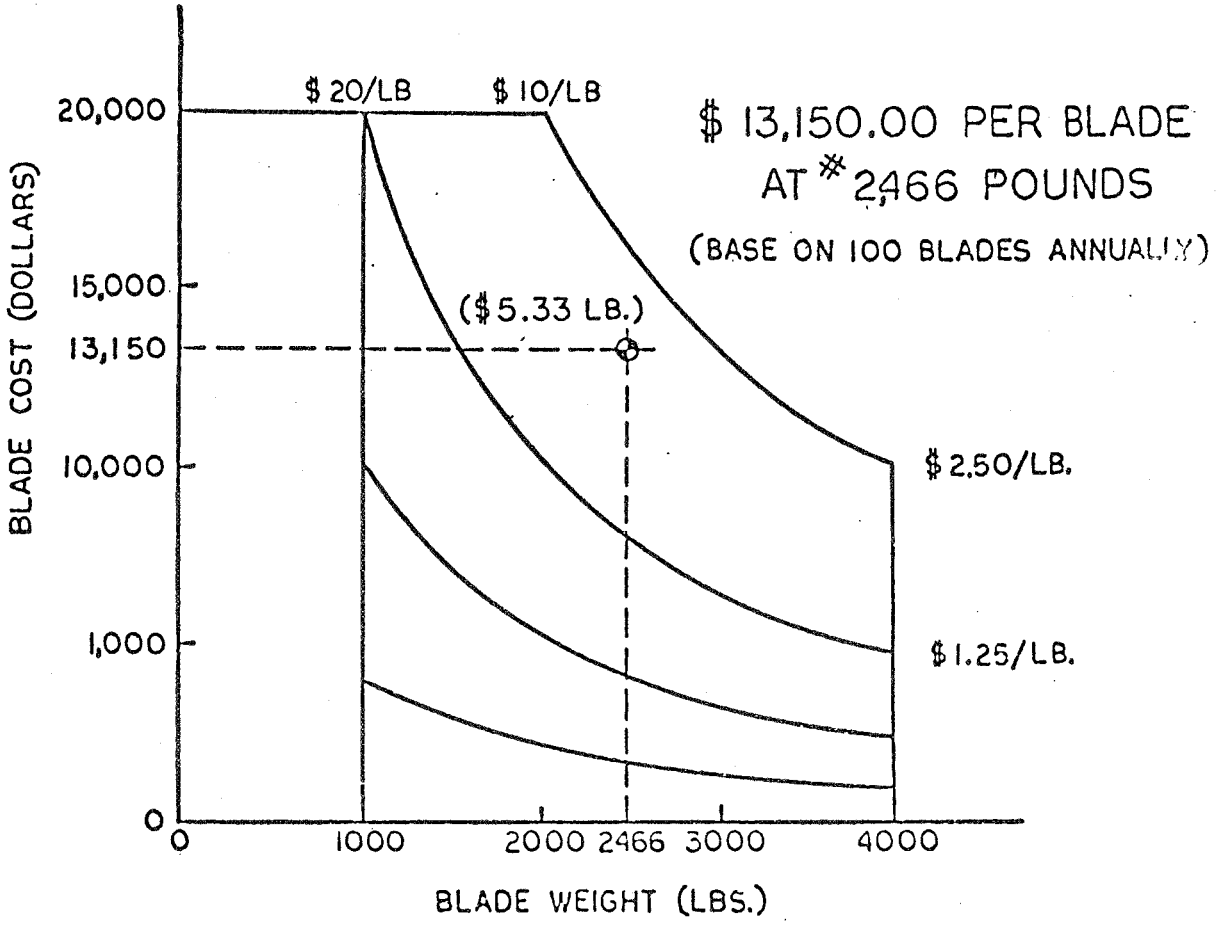

COST VERSUS WEIGHT DIAGRAM
(COST CURVES FROM BASIC N A S A DATA)

FIGURE 15 - COST SUMMARY

PRELIMINARY DESIGN REVIEW

Task I of the contract consisted of the development of a preliminary design using the stainless steel/fiberglass-foam blade concept. Various designs were reviewed, configuration studies were made, and a preliminary design was completed. This effort included several design iterations to establish the applied loads for the blade, which are a function of the mass distribution of the blade and the blade configuration. A study of available fatigue data and material properties was made.

To supplement the Budd Company experience, a subcontract was released to the Piasecki Aircraft Corp. for review and comment on the design concept.

Processing and tooling studies were made and a cost study of the preliminary design was completed. The following data and reports were submitted as part of the preliminary design activity:

1. Basic structural and mass distribution of the structure for the preliminary blade design
2. The Budd Company's investigation on the fatigue strength of spot welded joints in structural stainless steel
3. A study of rigid polyurethane foam
4. Piasecki Aircraft Corp. Report
5. Structural analysis for preliminary blade design
6. Preliminary fatigue properties of materials and connections to be used in the Budd Windmill blade
7. Preliminary cost estimate based on 200 units per year
8. Preliminary design review report
9. Preliminary design review presentation
10. Engineering drawing package

The preliminary design review was held at NASA-Lewis Research Center. The proposed blade design was approved. The review panel suggested that the following information be provided to NASA-Lewis prior to the final design review.

a) Analyze in detail all adhesively-bonded joints in the primary and secondary structures.

b) Analyze in detail all spot welded joints between the components of the spar.

c) Analyze in detail the complete structural properties of the spar and fiberglass-foam bodies.

d) Provide a detailed test plan(s) for qualification of all of the spot welded and adhesively-bonded joints.

To the extent possible within the scope of the contract, these items were addressed in the final design.

FINAL DESIGN PROGRAM

The final design program completed a final design of the blade developed during the preliminary design program (Task I); the final design program consisted of four principle tasks.

a) Task II, the first activity of the final design program contained the fatigue testing and other material evaluations required to verify the design stress levels for the final design, the design layouts, the structural analysis, and the design and fabrication of the 20 foot full scale root end test spar.

b) Tasks III and IV covered the fabrication procedures, cost analysis, and additional studies to apply the design concept to various size blades.

c) Task V was the preparation and presentation of the final design to NASA-Lewis Research Center and the preparation of the final report.

d) The results of the final design program are summarized in this section of the report. The fabrication of the spar test element is discussed separately following this section.

TEST PROGRAM

As mentioned earlier, the achievement of a thirty year life requires the careful selection and evaluation of materials. The design operating speed of the Mod-OA wind turbine is 40 rpm, which represents approximately 400 million cycles of loading during the thity-year life of a blade. It would be prohibitively costly to perform fatigue tests for 400 million cycles; therefore, it was necessary to use a more practical approach, similar to what other people have assumed. We assume that the fatigue strength at ten million cycles is equivalent to the endurance limit. In other words, we assume the S/N curve is flat by ten million cycles. Also, since few tests were performed, we took the lower limit of the test data as a measure of "test value" and 80% of that value as the "design allowable strength".

Considerable difficulty was encountered in developing a design for the end connections for the full scale test elements. Many early specimens failed prematurely at the pin connection of the specimen to the test machine.

The high stress levels achieved on the test configurations contributed to the problem. The solution to the end connection problem incorporated a split bushing arrangement with through bolt to provide a friction bearing clamp to carry the test loads. The design developed is shown in Figure 16.

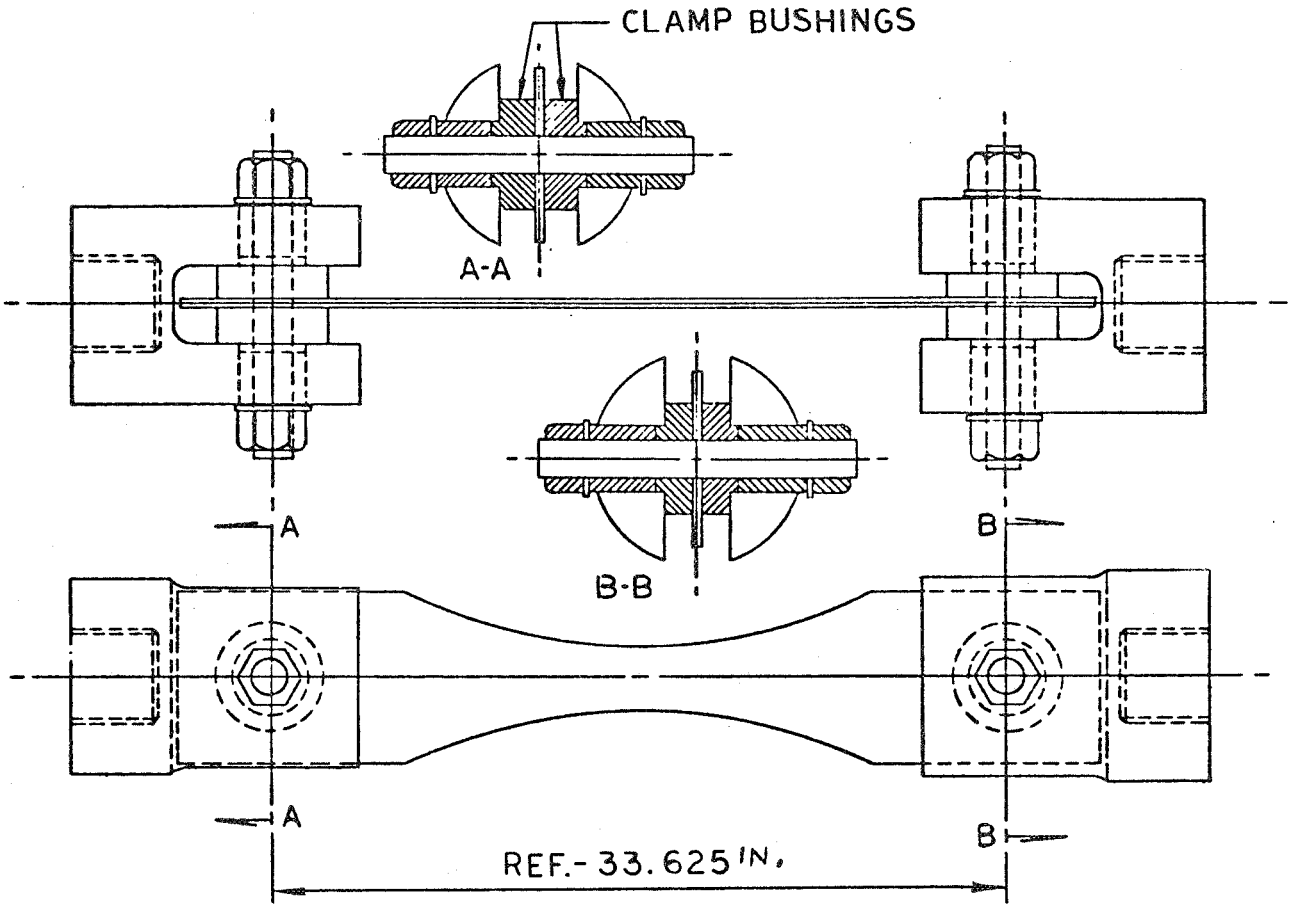

FIGURE 16 - TYPICAL FATIGUE SPECIMEN CONFIGURATION

The logic applied to the test program required that we conduct satisfactory fatigue tests for the base material and each joint configuration used in the design and that this data would be used to provide final sizing of the spar structural elements.

Some difficulties were encountered on two of the preliminary design joints. The base line design had a bolted and bonded root end attachment of the spar to root fitting. The use of mechanical fasteners was not a successful design, due to the stress concentrations generated by the first bolt in the load system. The design was changed to a welded connection that was satisfactorily fatigue tested. The other area of the base line design that had to be changed was the method of stopping off the reinforcement angles in the corners of the spar. It was found by testing that it was not possible to eliminate the stress concentration on the last spot weld at the end of the reinforcement. Therefore, the angles were tapered and extended the full length of the spar to eliminate the stress concentration. To improve the mass distribtuion in the spar, the reinforcement angles were butt fusion welded in two places allowing a reduction in the gage thickness outboard on the spar.

To supplement the full scale test elements, The Budd Company, using its own funds, conducted an independent test program to obtain long term fatigue data for the 301 1/4 hard material, including fusion welding as well as spot welding. The results of this activity were used to provide additional data for the blade design. Previous Budd Co. data was limited to approximately 2 million fatigue cycles. It was necessary to extend this data to 10 million plus load cycles to determine if the S/N curve was essentially flat beyond 10 million cycles. This was accomplished to our satisfaction, and the data was adjusted by use of modified Goodman diagrams to the proper R value and applied to the spar design. The data marked by an * on Figure 17 was obtained from the Budd supplemental program.

The data from the fatigue testing indicates that the knee of the S/N curve occurs at less than 4 million cycles for both the material and joints used in the design. This data supports our premise that 10 million cycles of fatigue testing is sufficient to predict long-term durability for the product.

Some of the tests were run for more than ten million cycles. The design allowable strength was defined as 80% of the test strength to allow for possible scatter. Also, the design allowables for other R values was established by using the Goodman Diagram.

There are five principle joint designs in the spar. A summary of the test results are shown in Figure 17. The data from the fatigue test program was presented at the final design review meeting and was included in the final design review report submitted to NASA.

TEST PROGRAM CONCLUSIONS
OF 301 1/4 HARD STAINLESS STEEL AND 4130 STEEL
SUMMARY OF TEST LEVELS AT 10 MILLION OR MORE LOAD CYCLES
ADJUSTED FOR "R" VALUE OF -.5

TEST	ADJUSTED TEST VALUE SHOWN IN CYCLIC STRESS	DESIGN ALLOWABLE (80% of ADJUSTED TEST VALUE)
BASE METAL (301 1/4 H STAINLESS STEEL)	* ± 49,000 psi	± 39,200 psi
BASE METAL (BUTT ARC WELDED & COLD WORKED) 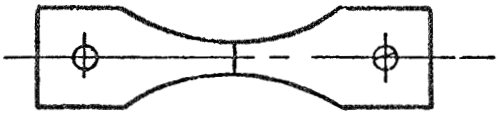	* ± 24,000 psi	± 19,200 psi
BASE LINE SPARE -SPOT WELDED (3 LAYERS) 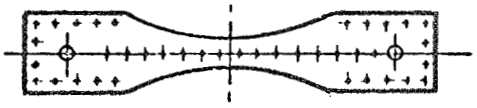	± 21,000 psi	± 16,800 psi
MAX SHEAR LOADS IN SPOT WELDS (R=+.1) 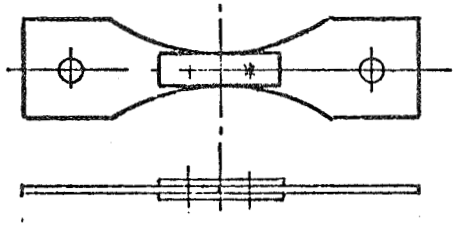	* ± 562.5 (CYCLIC LOAD PER WELD) SINGLE SHEAR	± 450 (CYCLIC LOAD PER WELD) SINGLE SHEAR
ROOT END ATTACHMENT - ARC WELDED 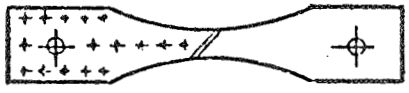	±16,000 psi 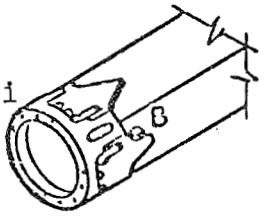	± 12,800 psi
A-TEST LOAD DETERMINED BY STRESS LEVELS AT AREA "A" B-AREA REPRESENTED BY TEST SPECIMEN		
4130 CHROME MOLY STEEL	± 38,000 psi (CHART VALUE)	± 30,400 psi

FIGURE 17 - TEST PROGRAM CONCLUSIONS

The fiberglass leading and trailing edge assemblies that form the aerodynamic surfaces were tested as a complete system by fabricating a one foot wide section representative of Sta. 187 inches on the blade. The maximum aerodynamic load was simulated by bonding masses to the outer surface of the test element which was then cycled on a shaker test fixture at resonance of the specimen. Figure 18 shows the test specimen and Figure 19 shows the test setup.

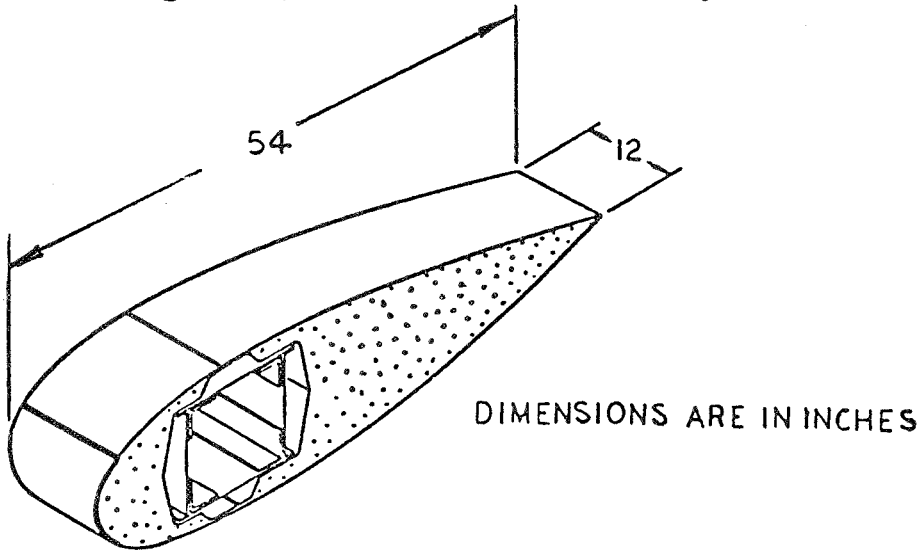

FIGURE 18 - TEST SPECIMEN AERODYNAMIC SURFACE

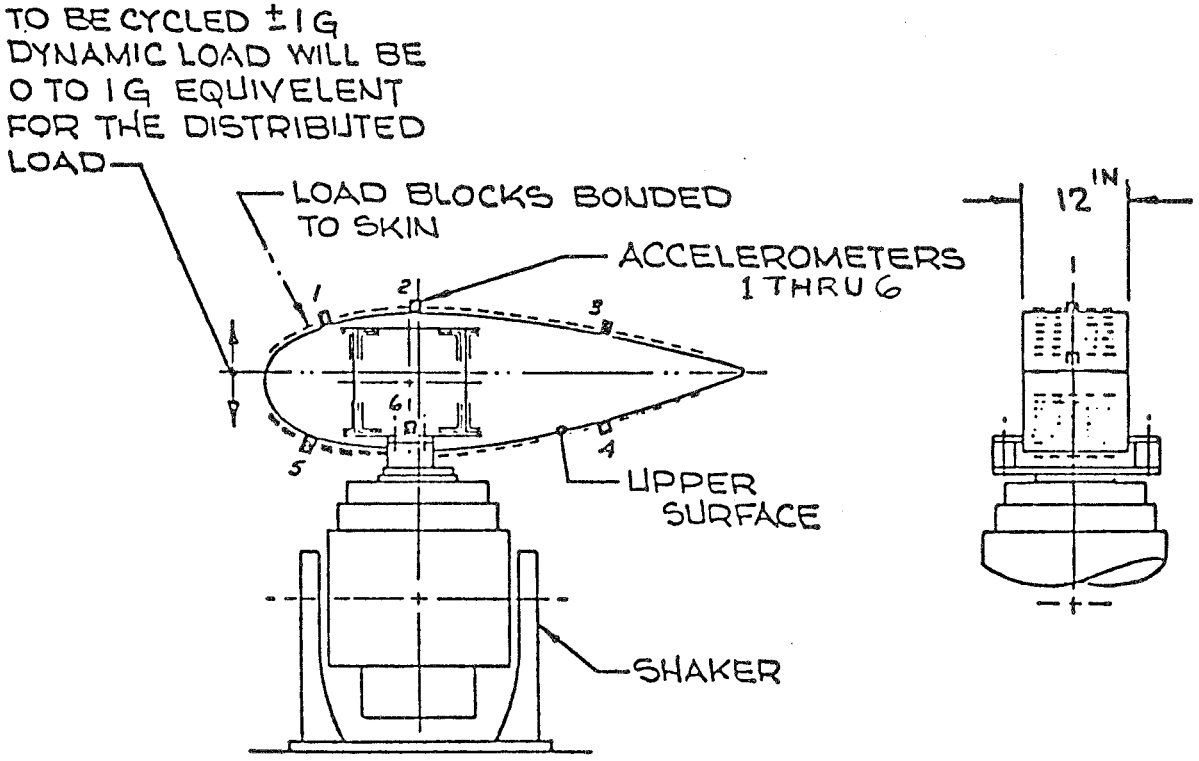

FIGURE 19 - AERODYNAMIC LOADING OF BONDING SURFACES

It was required that the blade sustain an ultimate load of 50 pounds/sq.ft. on the aerodynamic surfaces. To demonstrate this capability, a static test was performed. Figure 20 shows the test method. Sand bags were used to load the specimen.

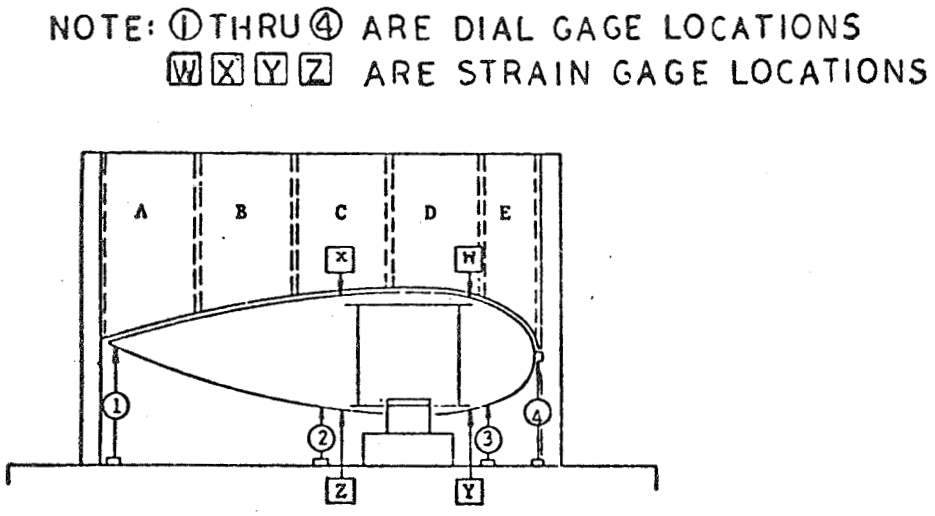

FIGURE 20 - STATIC LOAD TEST (CONFIGURATION)

The aerodynamic surfaces are constructed from the following materials:

Basic Material	Glass Reinforced Polyester with 17% minimum glass content
Trailing Edge Skins	.030 inches Commercial Sheet (as above)
Leading Edge Skins ..... and Inner Channels	Commercial Lay-up (.060 to .125 inches)
Foam (2-1/2 lb. Density)	Rigid Urethane Foam (Mobay Chemical Co. NB-2379 36A)
Adhesive	3-M Two Component Adhesive (EC-3549 BA)

The following is a summary of the results of the test program for the aerodynamic surfaces.

FATIGUE TEST

Test #1

Aerodynamic load equivalent from 0 to design max.
Mass load equivalent from 0 to 2 G
Tested at resonance (approx. 18 cycles per second)
Tested to 11,000,000 cycles (no failure)

Test #2

Aerodynamic load was increased to -1 to +2 x design max.
Mass load was increased to -2 to +4 G
Tested at resonance (approx. 18 cycles per second)
Tested to 1,100,000 cycles
(Induced minor failure in urethane bond to spar)

STATIC TEST

Static Design Load 50 lbs. per sq. ft. Proof Load

Conducted without repair

Test 1 - Loaded to 175 lbs. per sq. ft. (no failure)

Test 2 - 24 hr. Creep Test at 175 lbs. sq. ft.
(no creep)

The test program indicates that the design for the fiber glass aerodynamic surfaces is more than adequate for the design. Some weight reduction could be made although this is difficult due to process limitations.

Supplemental tests were run to evaluate the static ultimate strength of the bond between the foam core material and the skin (see Figure 21) and the ultimate strength of the aerodynamic surface bond to the spar and its elastomeric characters. See Figure 22.

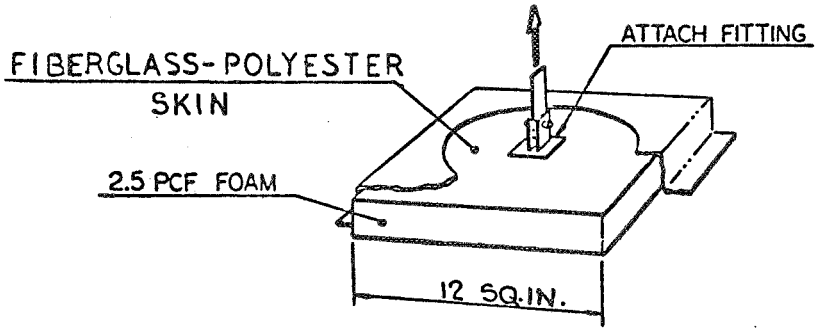

SKIN TO FOAM CORE (1ST FAILURE)
PULL STRENGTH 35 LB/SQ INCH
TEST CONTINUED TO SEPARATION OF SKIN & ATTACH FITTING (URETHANE BOND)
PULL STRENGTH 137 LB/SQ INCH

FIGURE 21 - SKIN TO FOAM PULL STRENGTH TEST

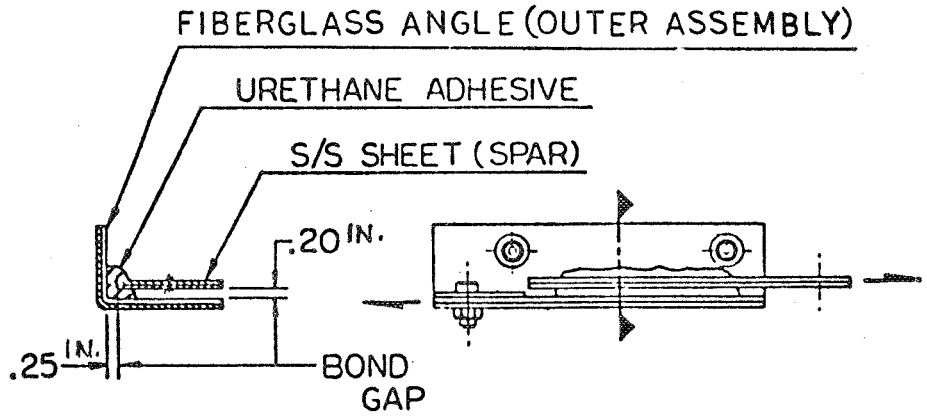

BOND TO STAINLESS STEEL ~ 1,340 LB./SQ. IN. (NO FAILURE)
BOND TO FIBERGLASS ~ 847 LB./SQ. IN. (FAILURE)
DEFLECTION AT FAILURE ~ 0.3 INCHES

FIGURE 22 - ULTIMATE LOAD SHEAR TEST (BOND OF THE SPAR TO AERODYNAMIC SURFACES)

Data for the design allowable to be used for the skin (.060 inches polyester fiber glass cloth sheeting) for the tip extension is taken from the Military Handbook MIL-HDBK-17 date November 5, 1959, Plastics for Flight Vehicles, Part I - Reinforced Plastics. Based on an ultimate strength of 30,000 psi per square inch from the handbook and a maximum design calculated mean stress of 3,600 psi and a cycle design stress of 1,900 psi the allowable stresses shown in Figure 23 can be determined.

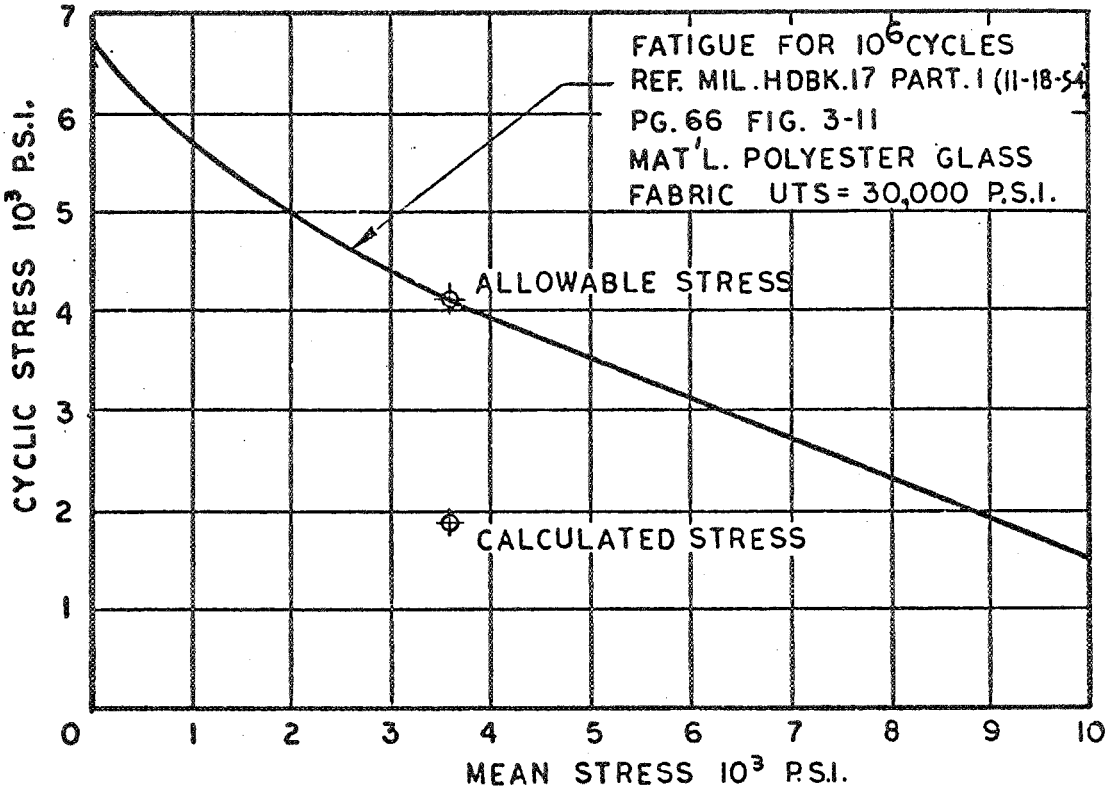

FIGURE 23 - FATIGUE FOR 10^6 CYCLES (POLYESTER GLASS)

In conclusion, we believe that we have accomplished a highly comprehensive test program, considering the limited funding available. Many developmental tests were conducted in all areas to provide the summary data.

STRUCTURAL ANALYSIS

Upon completion of the test program, the preliminary design was modified to be consistant with the test data. This included the change to a welded attachment of the root fitting and modification of the spar reinforcement angles to run the full length of the spar. The first iteration of the mass distribution was run on the MOSTAB computer code by NASA-Lewis to establish revised loads. Stress levels were developed from these loads and a second design iteration was made which reduced the mass of the spar and moved the center of gravity closer to the root end.

The feasibility of these modifications was demonstrated by the results of the 301 test program (which is discussed in Section on Test Program) - particularly the fatigue strength of butt fusion weld splices, which permits the reduction of the gage of the spar plates from .125 to .093 to .060 inches in three steps proceeding on board.

The mass distribution on this design was run on MOSTAB at NASA-Lewis and resulted in reduced loads in both axes of the spar. At this time, although the design met the contract requirements, NASA-Lewis reported that the design could not be run on the Mod-OA system unless the root end mass bending moment could be reduced to 47,000 ft. lbs. due to limitations established from experience gained running these machines.

The design was modified to meet the new NASA guidelines by shortening the stainless spar and providing a light-weight fiberglass tip extension from Sta. 650 to the outboard end of the blade. This modified mass distribution resulted in a mass moment for the final design of under 46,000 ft. lbs. The mass distribution for this design was run on MOSTAB by NASA-Lewis. Final loads were established and the analysis of the design was conducted using that data. Figure 24 shows the mass distribution on the blade.

Figures 25 and 26 show the edgewise and flatwise bending moments supplied as the output of the NASA MOSTAB run. These curves specify the steady and cyclic moments and therefore represent the fatiguing loads for the analysis and design of the spar. The blade planform and section along the span determined the chordwise spar location for the best combination of bending and polar moments of inertia.

The foam core and fiberglass skin which comprise the leading and trailing edge structures were designed and analyzed using data from the NASA curves showing the chordwise load distribution. The magnitude of the loads on the leading and trailing edges were determined from the above flatwise bending moment curves by measuring the slope of such curves at any given station. Thus, the slope at stations bracketing a desired location gave the difference in shears, which is the load within this portion of the span. The load, for twelve inches of span, was then distributed chordwise on the design. A full size test model of the twelve-inch width section was made for Sta. 187 and successfully survived the fatigue tests which simulated actual loading of the blade.

The stainless steel spar was located with its centroidal axis around the 30% chord in order that the maximum depth shall be realized. During stages of the design effort, fatigue allowables for stainless steel sheet and spotwelds were used for sizing the spar sections so they may endure the flatwise and edgewise bending moments. Goodman Diagrams were constructed for representing these fatigue allowables. The most critical portion of a typical section of the spar appeared near the extreme corners where spotwelds attached the upper and lower plates to the vertical webs. This is shown schematically in page 43 as the "spar final connection assembly".

At any given station, the steady and cyclic bending moments were known about each principal axis and therefore the mean and cyclic stresses at any point within the spar section became the algebraic sum of like stresses (steady or cyclic) produced by each bending moment. The system of reinforcing members was designed to assure that each spar section would have sufficient properties to keep stresses within reasonable values for minimum weight. As the design progressed, Budd testing of stainless steel specimens and spotwelds provided more current fatigue information which was immediately employed so that stresses remained within the newly-constructed Goodman Diagram.

Initially, the stainless steel spar extended to the outer tip with a minimal section at very low stresses from Sta. 650 outboard. This suggested the use of a complete fiberglass foam assembly without the stainless steel spar. Analysis indicated that the fiberglass skin provided enough section properties to resist fatigue stresses caused by the outboard bending moments. The flatwise mode was most critical for stresses around the 30% chord at Sta. 650 and were maintained at levels far below fatigue allowables for fiberglass (see Figures 2 and 28). Edgewise moments produced stresses at the leading and trailing edges of low magnitude due to large section properties in the edgewise direction. In view of the conservative material allowables used for this portion of the blade, a great weight saving was still achieved through judicious design and analysis.

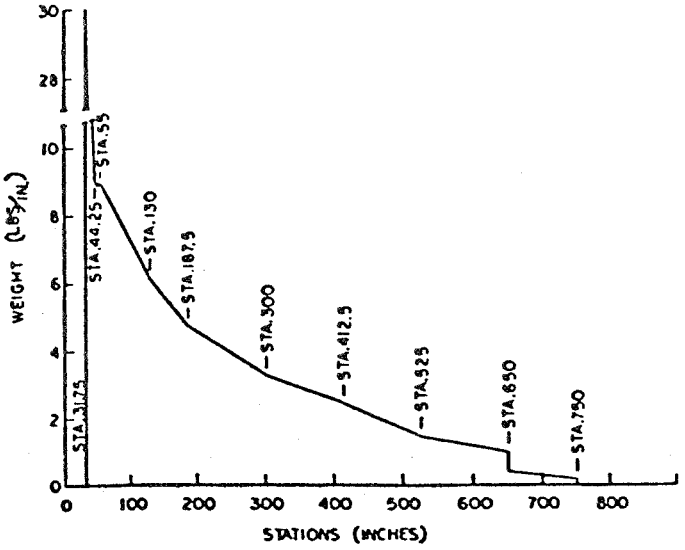

FIGURE 24 - BLADE MASS DISTRIBUTION

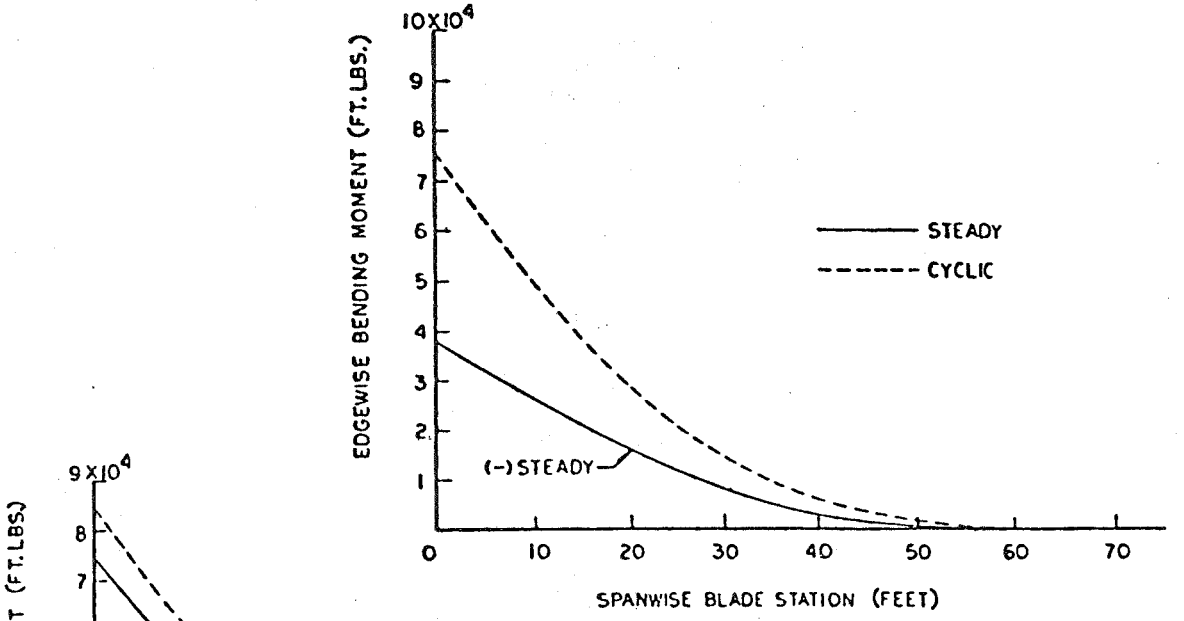

FIGURE 25 - EDGEWISE BENDING LOADS

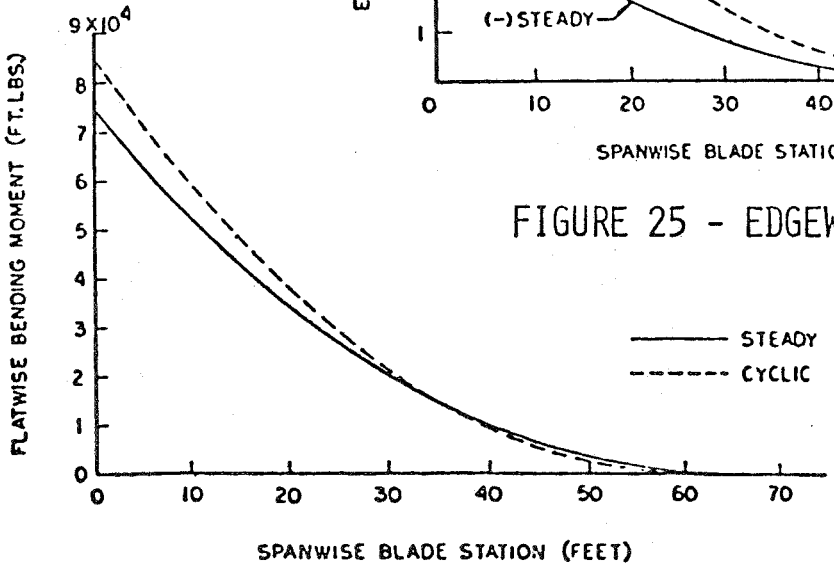

FIGURE 26 - FLATWISE BENDING LOADS

The spanwise moments of inertia of the spar were calculated and are shown on Figure 27.

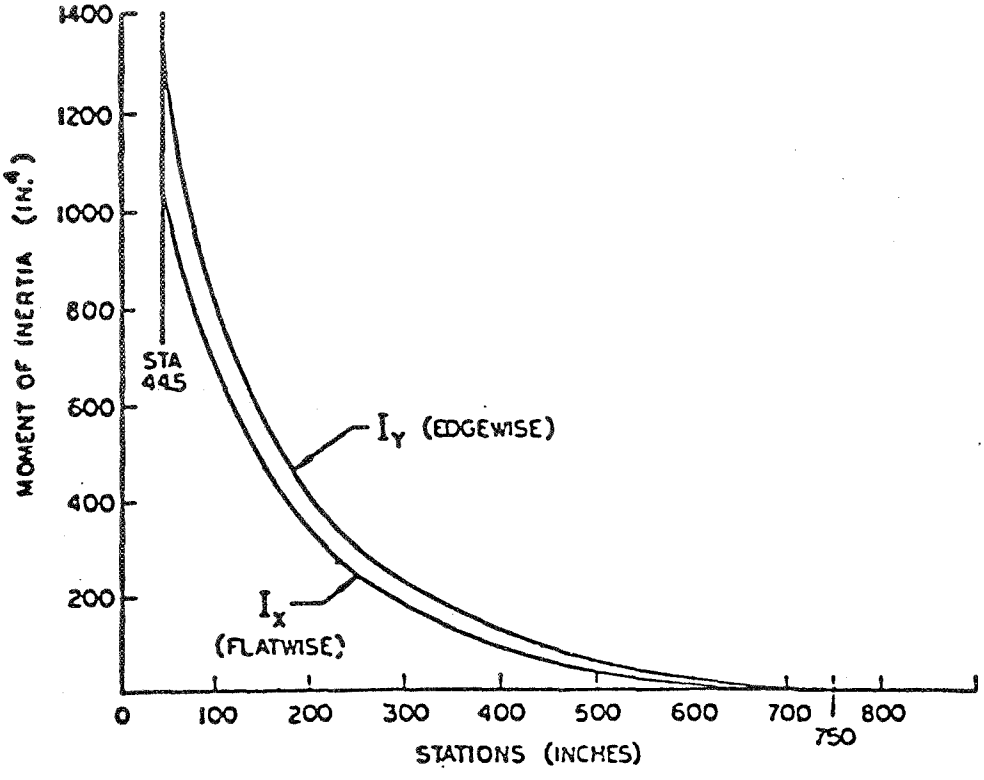

FIGURE 27 - SPAR MOMENT OF INERTIA

The chart shown on Table 1 is a summation of the calculated stresses developed in the spar.

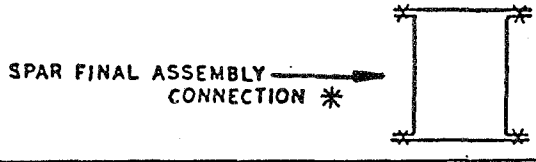

STA.	WEB	CAP	ALLOWABLE CYCLIC – STRESS(PSI)	MAX.COMBINED CYCLIC – STRESS(PSI)	MEAN STRESS(PSI)	MAXIMUM STRESS(PSI)	MINIMUM STRESS(PSI)	R = MIN./MAX.	SHEAR * FLOW (LB./IN)	MARGIN OF SAFETY
44.5	.125	.125	12,800	11,000	3,340	14,340	-7,660	-.53	103±13	16.4%
187.5	.125	.125	16,800	15,914	4,814	20,728	-11,100	-.54	102±18	5.6%
300	.090	.125	16,800	16,000	5,285	21,285	-10,715	-.50	104±32	5.0%
412.5	.090	.090	16,800	14,300	6,753	21,053	-7,547	-.36	85±32	17.5%
525	.060	.060	16,800	12,383	7,790	20,173	-4,593	-.23	73±35	35.7%
637.5	.060	.060	16,800	6,959	6,278	13,237	-621	.05	74±05	141.4%

TABLE 1 - SUMMATION OF STRESSES IN SPAR

The structural characteristics of the blade were run on a computer program at Budd and at NASA-Lewis and these predicted a flatwise natural frequency 1.86 hz and a edgewise natural frequency 2.15 hz. NASA-Lewis approved these values at the final design review.

Figure 28 shows a section of the tip extension at the area of highest bending stress.

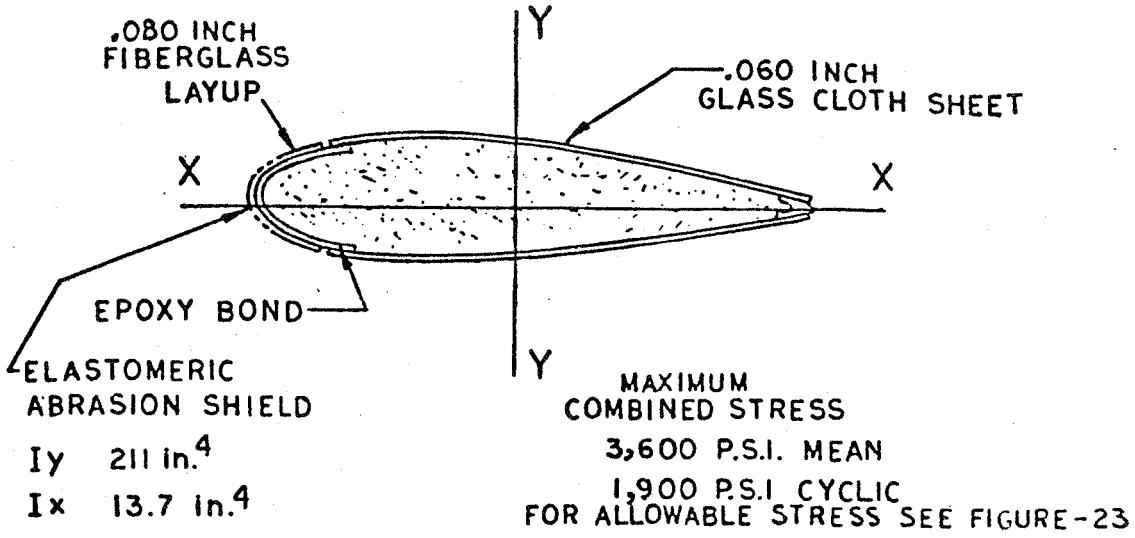

FIGURE 28 - SECTION FIBERGLASS OF TIP EXTENSION

The complete structural analysis was submitted to NASA-Lewis at the final design review. The full scale root end test beam was designed and the analysis was submitted during the final design review. The test beam will be discussed in more detail in the section on fabrication of the test beam.

COST AND WEIGHT ANALYSIS

We have made a cost and weight analysis of the blade design. The blade assemblies and parts were reviewed for manufacturing procedures and tooling and weights were determined. Figure 29 shows the basic configuration for the 62 ft. blade. A summary of the weight and cost of each major assembly, including tooling cost, is presented in Table 2. The costs are based on a production level of 100 blades per year. Figure 32 shows the cost summary of the blade design at 100 units per year and the relative cost of the blade versus the requirements established by the contract.

As can be seen, we fall well within the low cost objectives established by NASA-Lewis. Table 3 shows costs established to predict the approximate blade cost at various production levels per year. These values have been rounded off to simplify the numbers. The process work done and the tooling studies indicate the design is a practical low cost approach to wind turbine blade design.

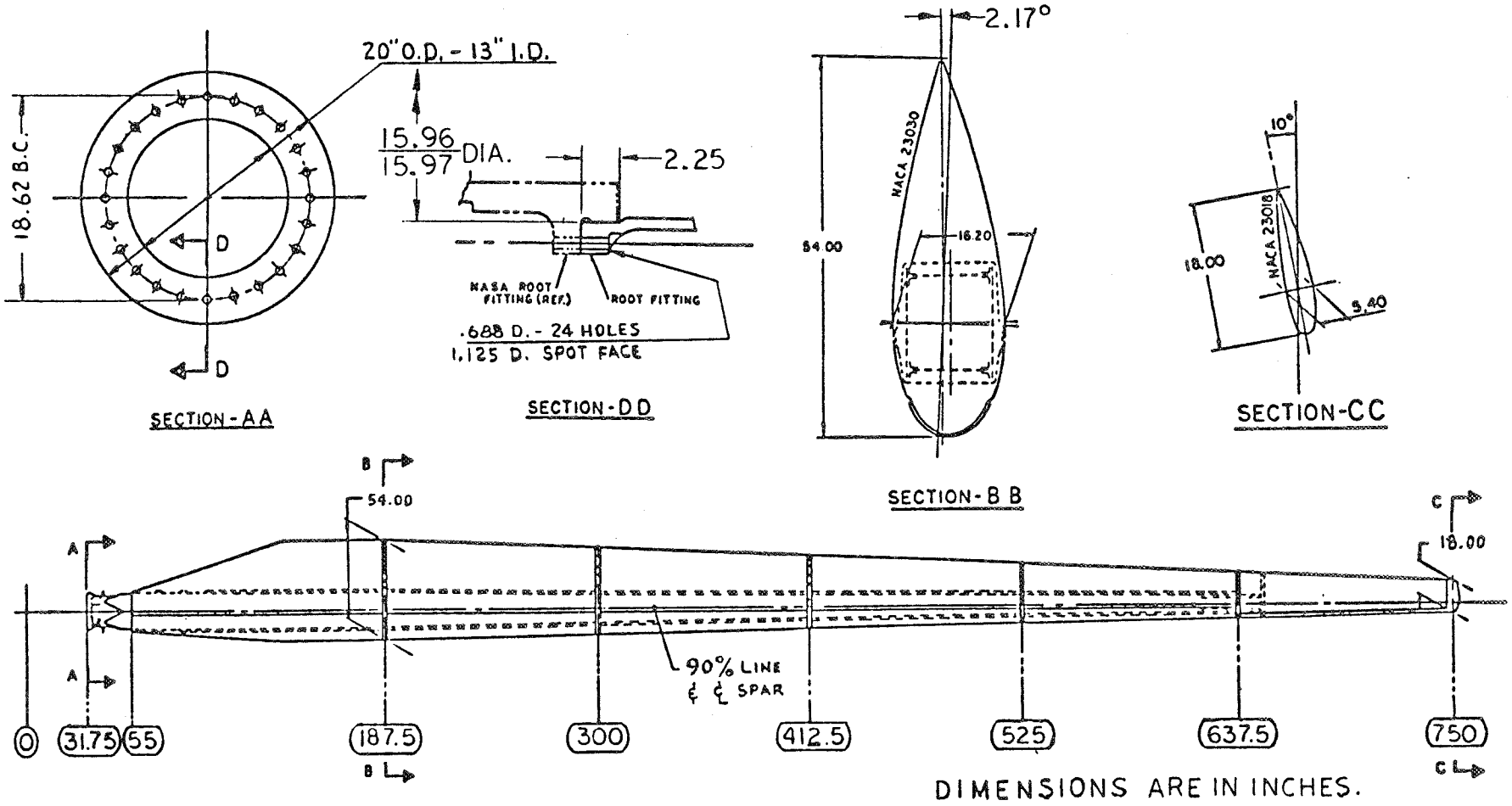

PLAN VIEW OF BLADE

FIGURE 29 - 62 FT. BLADE CONFIGURATION

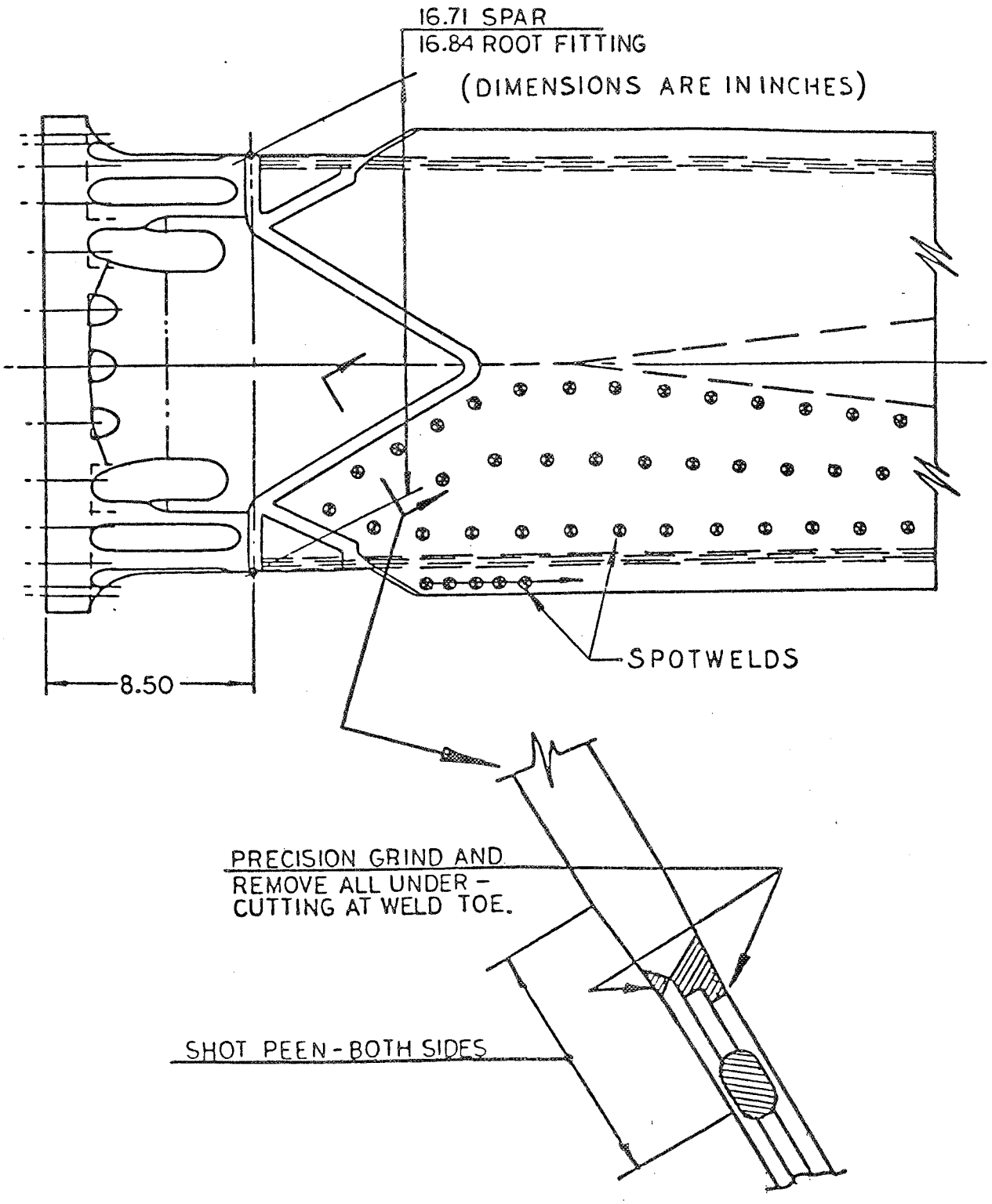

FIGURE 30 - ROOT END - SPAR CONFIGURATION

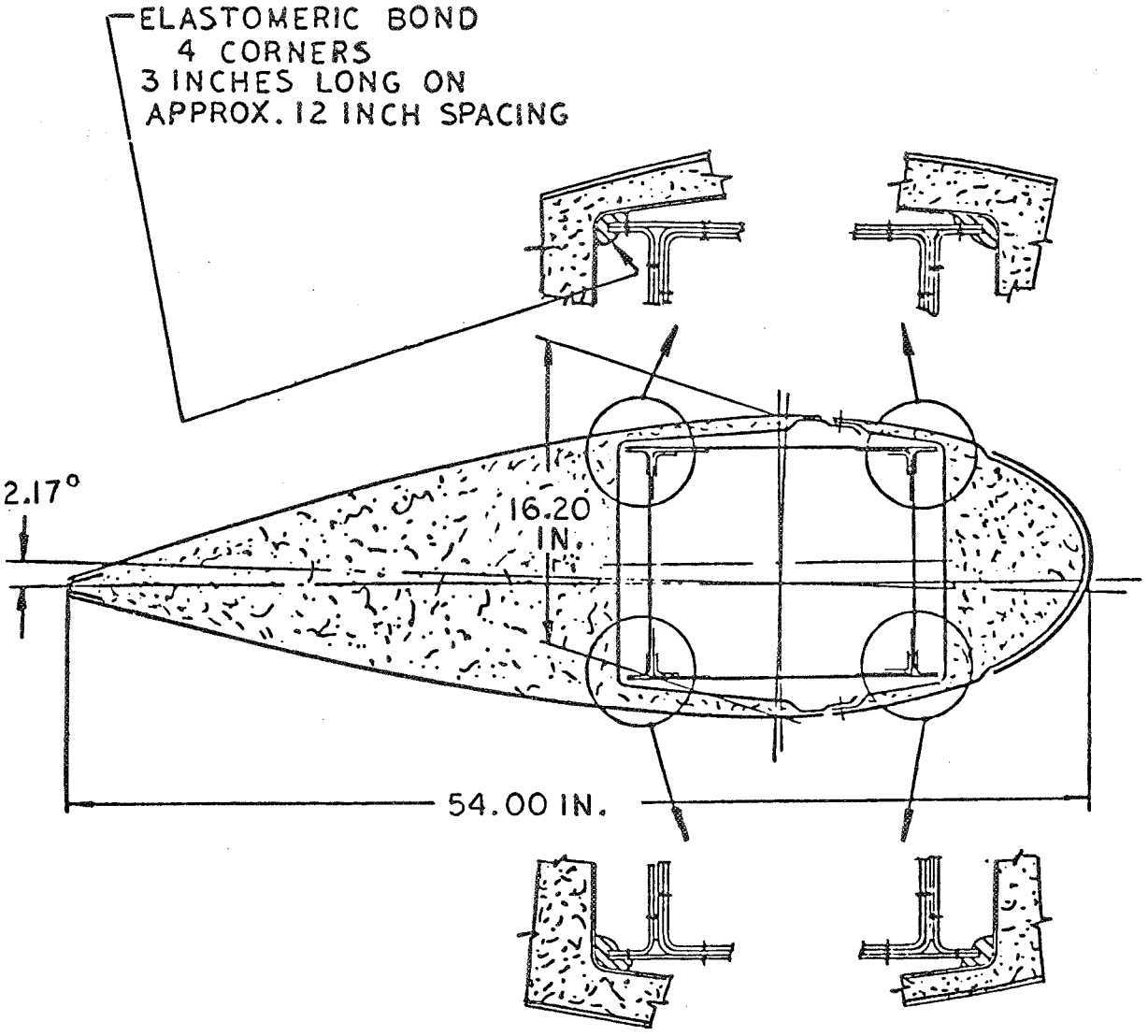

FIGURE 31 - SECTION THRU BLADE - OUTBOARD OF STATION 187.5

PART.NO.	DESCRIPTION	QTY	WEIGHT	MAT'L	LABOR	COST	TOOL COST
0518-100101	Spar Assembly	1	1635.7	2442	2904	5346	441,300
104	Trailing Edge Assy	1	86.4	222	176	398	54,500
105	" " "	1	66.6	173	172	345	50,800
106	" " "	1	55.1	135	150	285	45,500
107	" " "	1	45.3	114	141	255	40,300
108	" " "	1	33.4	84	128	212	36,000
121	Leading Edge Assy	1	73.6	287	86	373	41,000
122	" " "	1	52.7	253	86	339	40,000
123	" " "	1	40.9	170	75	245	34,000
124	" " "	1	30.9	138	66	204	30,500
125	" " "	1	21.5	107	60	167	27,800
126	Fiberglass Tip Assy	1	43.8	110	146	256	45,400
145	Joint Seal	5	12	10	-	10	-
146	Holding Brkt Boot	2	2	4	-	4	1,000
147	Upper Root Fitting Cover	1	7	24	5	53	5,200
148	Lower Root Fitting Cover	1	7	24	5	53	5,200
150	Spar Root Fitting Assy	1	1815.7	15	275	290	36,000
200	Root Fitting	1	180	169	396	565	66,000
	Adhesive	A/R	72.1	66	-	66	-
100	Blade Assy	1	-	53	704	757	219,700
TOTAL			2466	4600	5570	10170	1,215,000

TABLE 2 - COST ANALYSIS SUMMARY (BASED ON 100 BLADES ANNUALLY)

ESTIMATED COST SUMMARY
BASED ON 100 BLADES ANNUALLY

TOOL COST

Tools 1,215,000

Based on Production of 100 Blades Annually

Tool Cost 1,215 Per Blade

(Tools Prorated on 10 Years Production)

COST SUMMARY

Material	4,600
Labor	5,570
Tools	1,215
Total	11,385
5% G&A	570
Total Cost	11,955
10% Profit	1,195
Cost & Profit	13,150 Per Blade

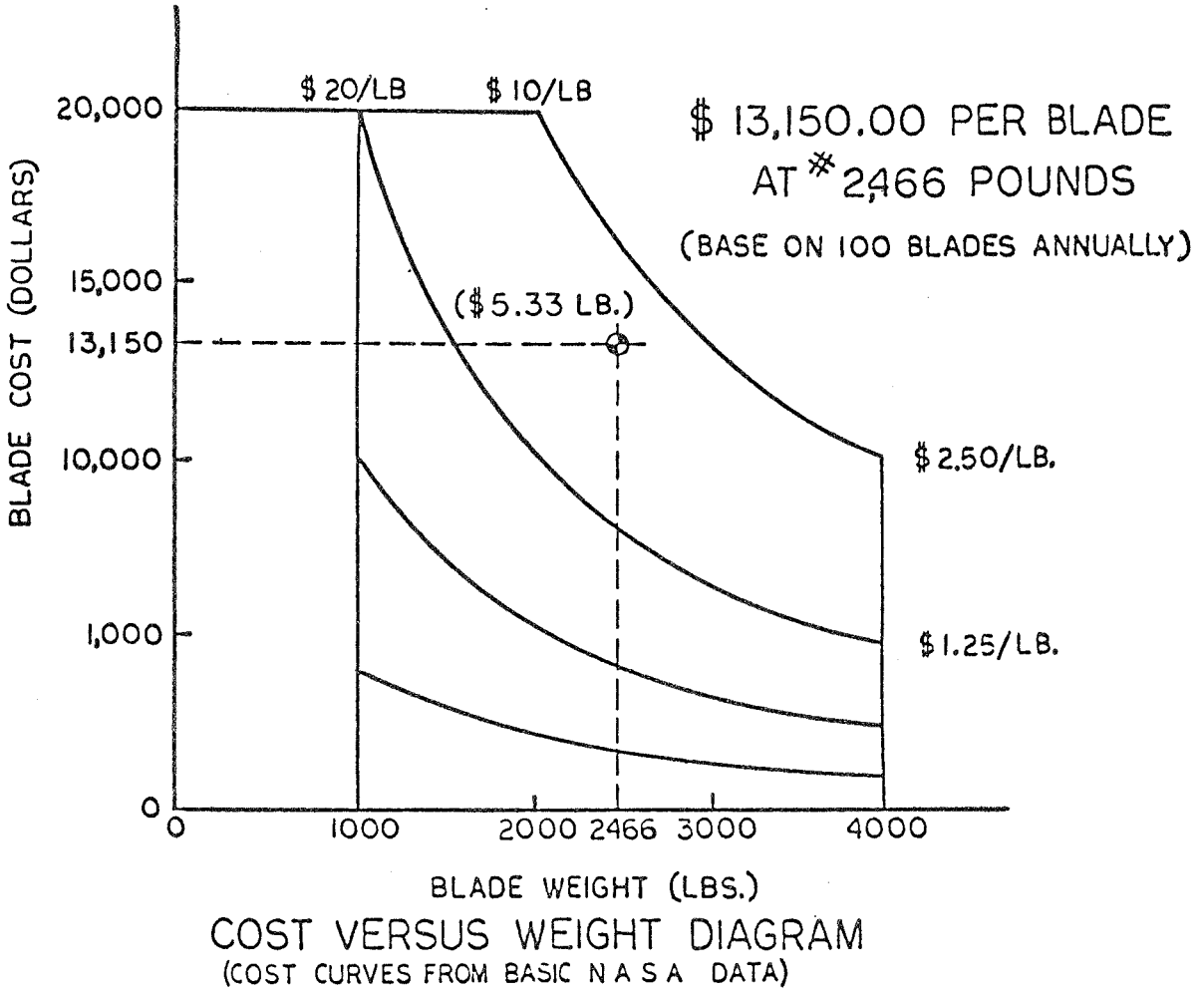

COST VERSUS WEIGHT DIAGRAM
(COST CURVES FROM BASIC N A S A DATA)

FIGURE 32 - COST SUMMARY

MANUFACTURING COST FOR VARIOUS BLADE QUANTITIES

COST CURVED FOR VARIOUS BLADE QUANTITIES
BASED ON 1978 DOLLARS

QUANTITY	COST PER BLADE (EXCLUDING TOOL COSTS)
2	$ 60,000
10	$ 40,000
100	$ 11,500
1000	$ 8,800

TOOLING COST BASED ON PRODUCTION TOOLS
FOR ALL QUANTITIES

PRODUCTION TOOLS	1,215,000
5% G & A	60,750
TOTAL COSTS	1,275,750
10% PROFIT	127,575
COSTS & PROFIT	1,403,325

TOOL COST TO BE AMORTIZED BASED
ON THE QUANTITY OF BLADES TO BE BUILT

NOTE: UP TO 20 BLADES THERE IS A COST ADVANTAGE TO USE PROTOTYPE TOOLS VS PRODUCTION TOOLS

TABLE 3 - MANUFACTURING COST OF VARIOUS BLADE QUANTITIES

SHIPPING AND HANDLING

A study was made to determine a practical means for handling and shipping the blades. Figure 33 shows the shipping fixture as visualized. We would consider shipping the blades either by truck or by rail. There would be a mounting fixture for the root end of the blade and a mounting fixture for the midpoint location of the blade. These fixtures are designed so that any deflection of either the trailer or the railcar flat bed would not put extraneous loads onto the blade during shipment. When shipping, the blades would be wrapped in polypropylene plastic material to protect them from the weather and vandalism. On railcar shipment, it would be desirable to have a gondola type car with high sides for protection. Figures 34 and 35 show the lifting provisions made at the root end and at the mid-spar point. The blade can be lifted vertically with the leading edge or trailing edge up and it can be lifted with the blade in the horizontal position. There are four lifting lugs on the root end fitting. The root end fitting at this location has been increased in thickness and the lugs are in a low stress area. Double lifting lugs are provided at the mid-blade point to provide capability of transfer from one lift system to a second lift system.

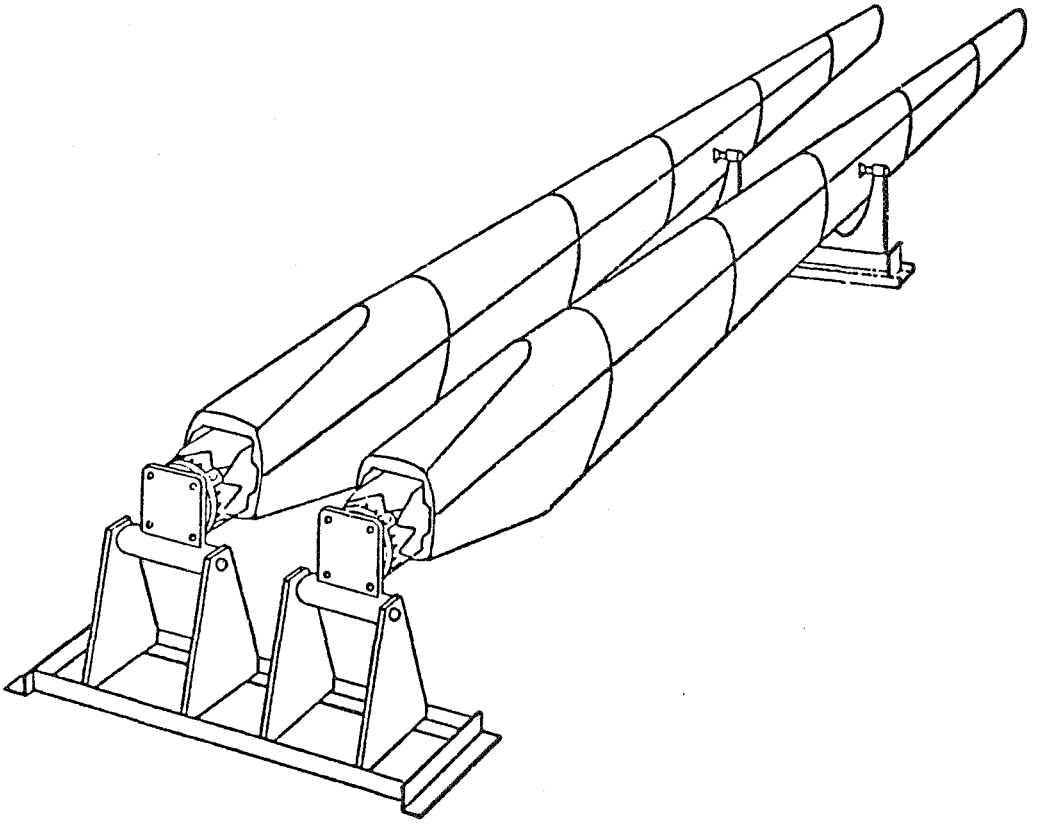

FIGURE 33 - SHIPPING FIXTURE ARRANGEMENT

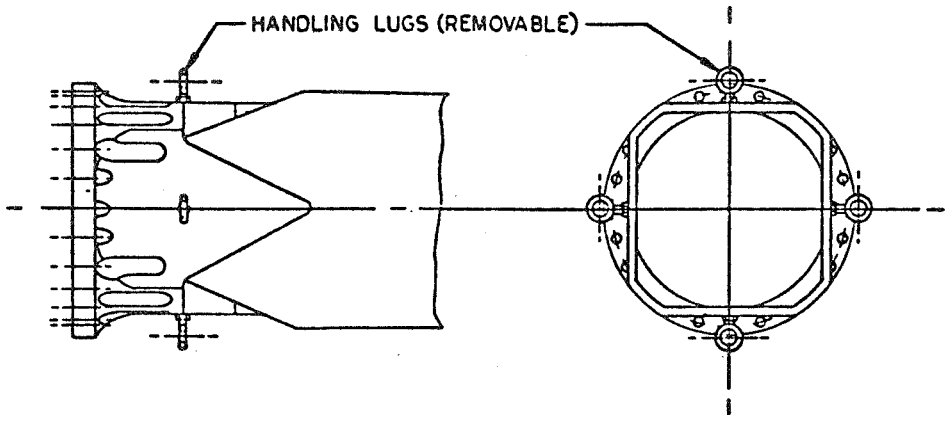

FIGURE 34 - ROOT END HANDLING POINTS

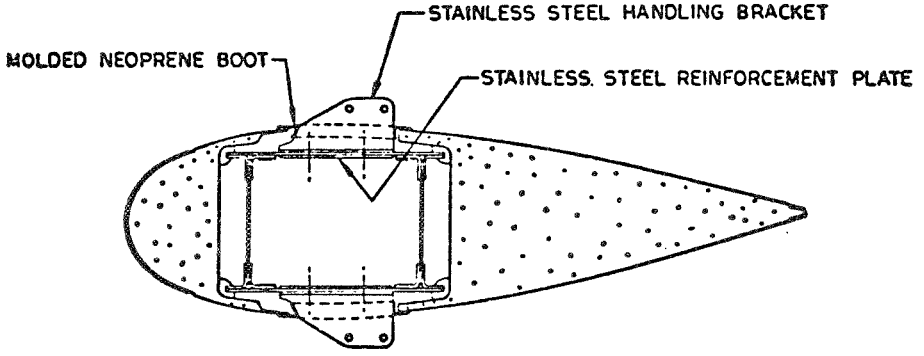

FIGURE 35 - BLADE HANDLING POINTS

FABRICATION OF THE SPAR TEST ELEMENT

To verify the spar design, a root end section of the spar was designed and fabricated. The test beam element is full scale and approximately 20 feet long. The root end welding and attachment is simulated exactly. Shown in Figure 36 is the design of the root end test beam.

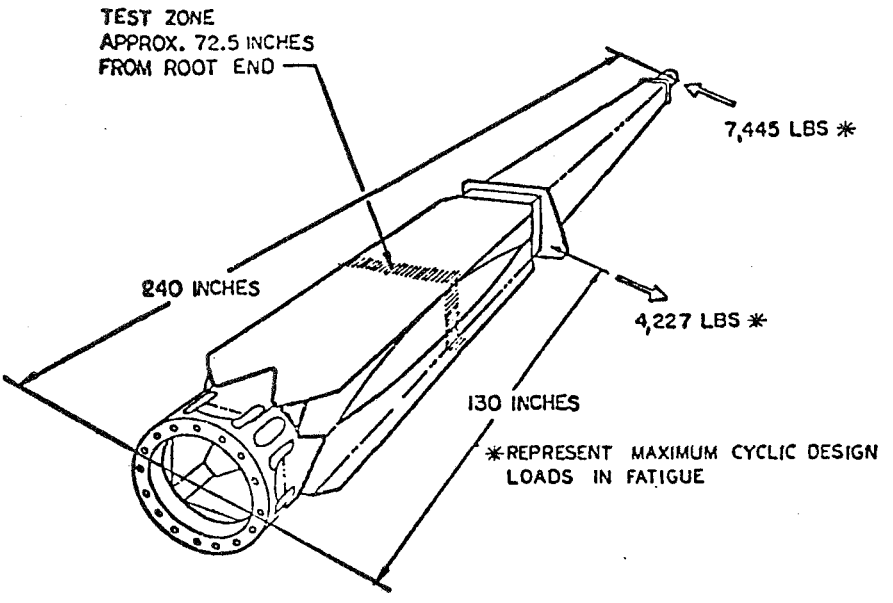

FIGURE 36 - ROOT END TEST BEAM

It is essential for testing a fabricated beam that the bending shear stresses be simulated in addition to the direct bending stresses. To accomplish this, we recommend that two opposing loads be applied to the beam as represented by Figure 36. This loading design will simulate correctly the combined direct and shear stresses at station 72.5 and the maximum bending moment at the root end attachment. Secondly, the design cycle loads correspond to an "R" value different than that of the planned test. The recommended loads were calculated on the basis of equal margins of safety for the test loads and design loads relative to the Goodman Diagram. The analysis of the test beam was submitted during the final design review.

Figures 37 through 45 show the beam at various levels of manufacture.

Figure 37 shows the extension beam assembly and its parts. This beam is used to extend the test beam to a length of 20 feet to match the NASA test fixture. The parts in the background are the spot weld and root end arc welding process certification assemblies.

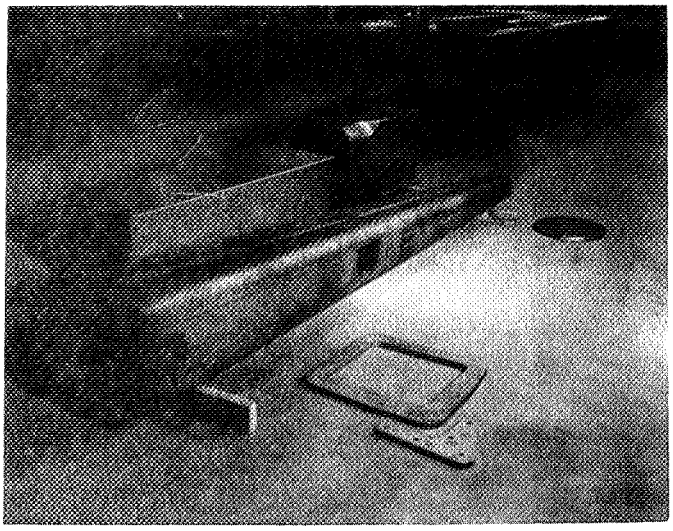

FIGURE 37 - EXTENSION BEAM ASSEMBLY AND PARTS

Figure 38 shows the inboard end of the side plate angle assemblies of the spar.

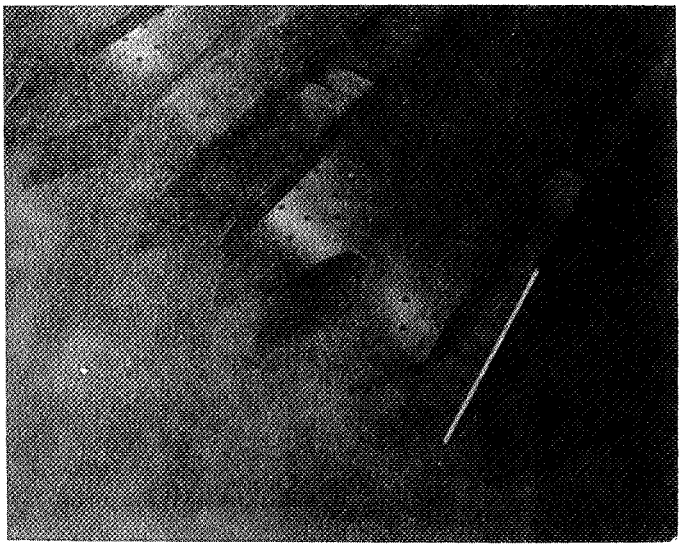

FIGURE 38 - INBOARD END OF SIDE PLATE ANGLE ASSEMBLIES OF SPAR

Figure 39 shows the temporary fixture used to assemble the test beam side and top plate assemblies. It is fabricated of aluminum and has adjustable fixture blocks to match the geometry of the top and side assemblies.

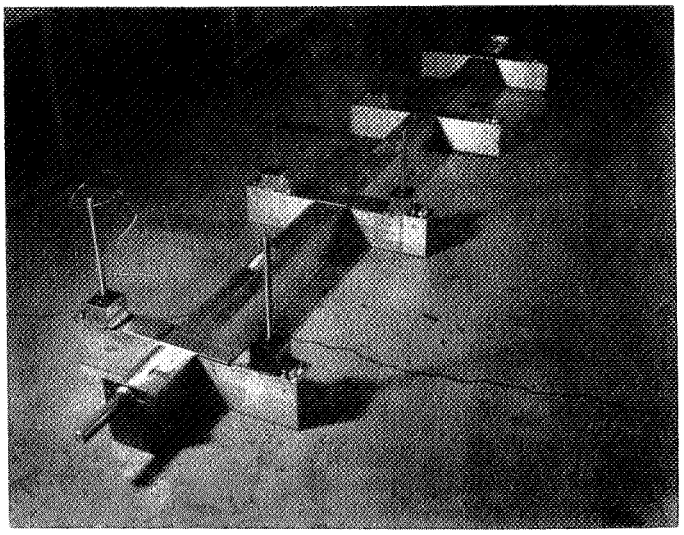

FIGURE 39 - TEMPORARY FIXTURE FOR TEST BEAM SIDE AND TOP PLATE ASSEMBLIES

Figure 40 shows the four assemblies completed, ready for assembling into the box spar.

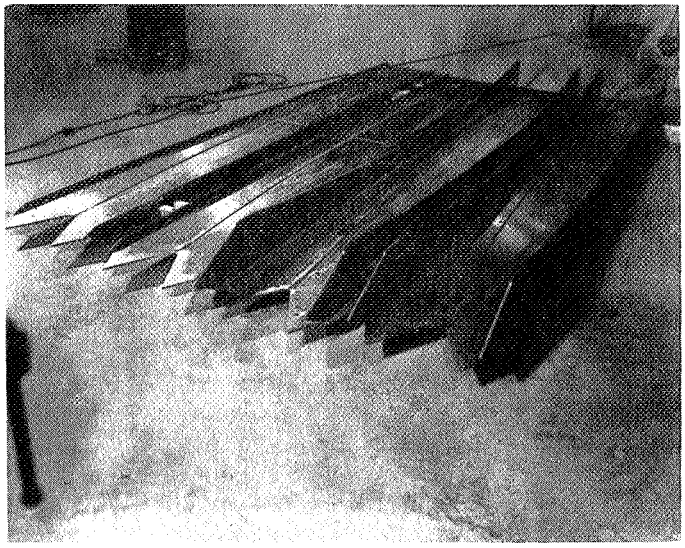

FIGURE 40 - FOUR ASSEMBLIES READY FOR BOX SPAR

Figure 41 shows the stainless steel spar assembled and the weld preparation prior to attachment of the root end fitting.

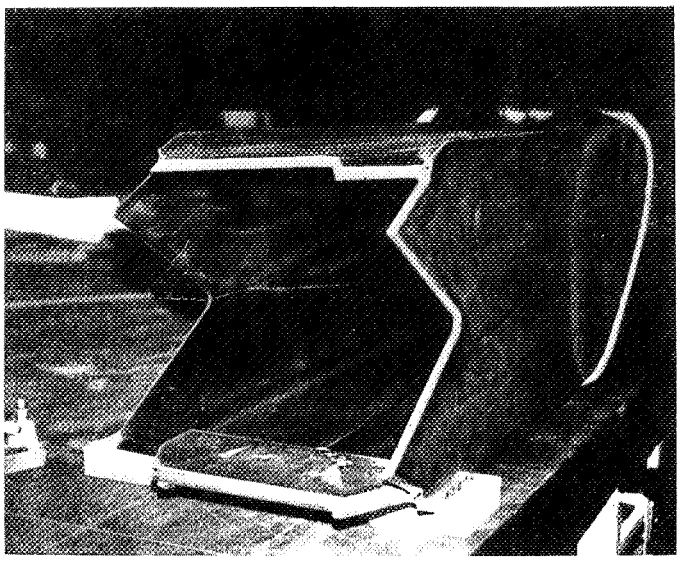

FIGURE 41 - ASSEMBLED BOX SPAR

Figure 42 shows the arc welding configuration of the 4130 carbon steel root end fitting to the stainless steel box spar. The weld was made by preheating the parts during the welding process. The weld has been ground, polished and cold worked on the surface to improve its fatigue resistance.

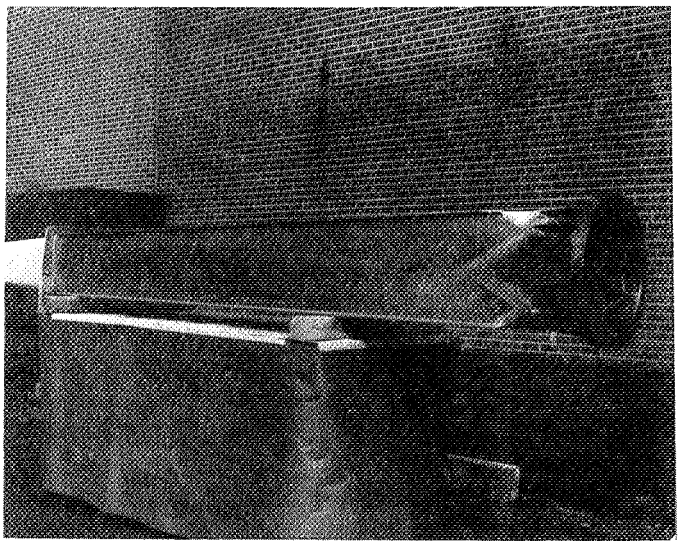

FIGURE 42 - ARC WELDING CONFIGURATION OF 4130 ROOT END FITTING TO STAINLESS STEEL BOX SPAR

Figure 43 shows the attachment of the carbon steel end extension and the stainless steel spot welded spar.

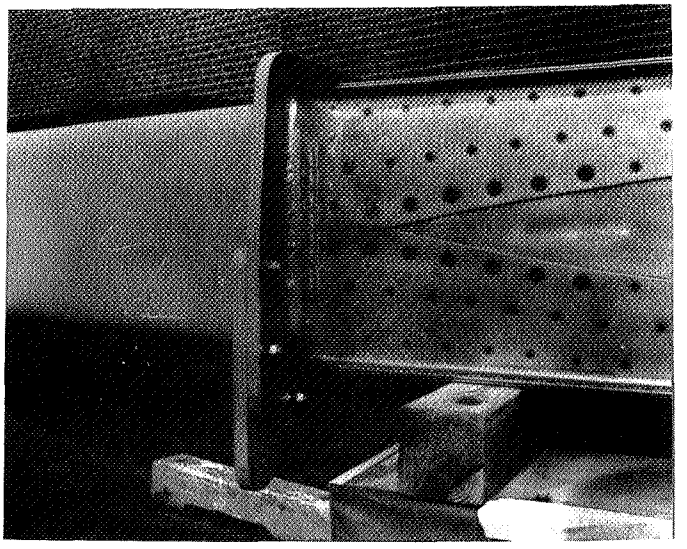

FIGURE 43 - ATTACHMENT OF CARBON STEEL END EXTENSION AND STAINLESS STEEL SPOT WELDED SPAR

Figure 44 shows the butt arc weld at the splice between the .125 inch to .090 inch web plate. The weld has been ground and polished and then cold worked to provide the high test allowable. This weld is located at the mid-point of the test spar, the area of highest stress developed in the spar test.

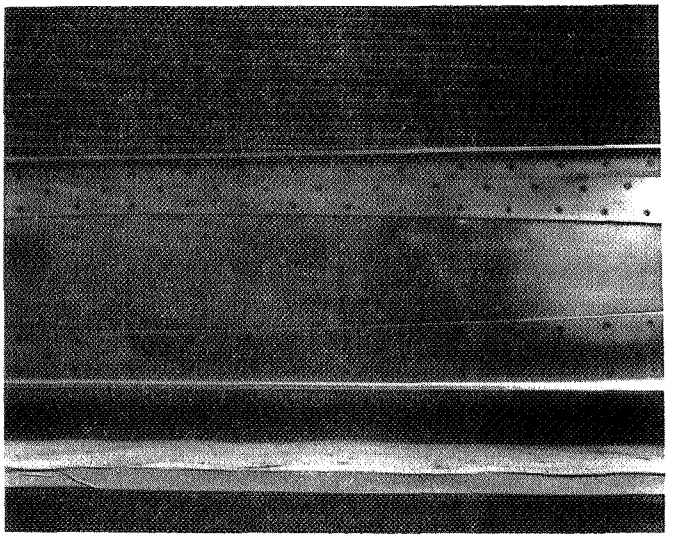

FIGURE 44 - BUTT ARC WELD SHOWN AT SPLICE BETWEEN .125 TO .090 INCH WEB PLATE

Figure 45 shows another view of the finished test beam (and anchor) before shipping.

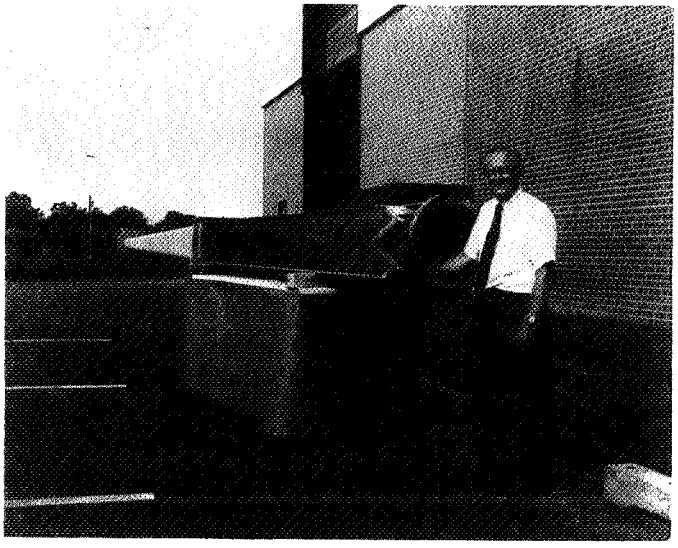

FIGURE 45 - TEST BEAM SHOWN BEFORE SHIPPING TO NASA-LEWIS FOR TESTING

During the manufacture of the test beam, all the processes required for manufacture of the spar for the 60 foot blade, were demonstrated and certified. The test beam was shipped to NASA Lewis for testing by the Government.

CONCLUSIONS

The test beam was fabricated and delivered to the Government. The fabrication of the test beam certified the processes used to fabricate the stainless steel spar for the blade. We are pleased with the product and believe the stainless design used for the spar has cost and weight advantages for wind turbine systems 125 ft. diameter and under. The large systems up to 300 ft. diameters would require a fusion welded low alloy carbon steel spar. The processes for this spar follows conventional industrial practice with the exception that more complete and exacting quality control procedures would be used for the fusion welding processes. The design of the aerodynamic surfaces was demonstrated satisfactorily with the system element test performed during the program. Additional analysis that was done for application to the large blades indicate that the Budd approach for fabricaitng and control of the aerodynamic surfaces is practical and lends itself well for the application.

It was concluded that the Budd blade concept is a viable design for application to large wind turbine systems. A complete design for a blade applicable to the MOD-OA system was accomplished and the blade design satisfies the NASA Lewis Research Center specifications. The design concept is applicable to various length blades. Blades less than 60 feet would use a stainless steel spar and blades of larger size would have a fusion welded carbon steel spar. The design permits a choice of a wide selectivity of air-foil shapes and, because of its modular construction, the design provides producibility and quality in high volume production.

1. Report No.	2. Government Accession No.	3. Recipient's Catalog No.
NASA CR-165491		

4. Title and Subtitle	5. Report Date
Design and Evaluation of Low-Cost Stainless Steel - Fiberglass-Foam Blades for Large Wind Driven Generating Systems	October 1982
	6. Performing Organization Code

7. Author(s)	8. Performing Organization Report No.
Walter S. Eggert, Jr.	
	10. Work Unit No.

9. Performing Organization Name and Address	11. Contract or Grant No.
The Budd Company Technical Center 375 Commerce Drive Fort Washington, Pennsylvania 19034	DEN 3-129
	13. Type of Report and Period Covered Contractor Report
12. Sponsoring Agency Name and Address U. S. Department of Energy Wind Energy Technology Division Washington, D. C. 20545	14. Sponsoring Agency ~~Code~~ Report No. DOE/NASA/0129-1

15. Supplementary Notes

Final Report. Prepared under Interagency Agreement DE-AI01-79 ET20320. Project Manager, R. F. Lark, Wind Energy Project Office, NASA Lewis Research Center, Cleveland, Ohio 44135.

16. Abstract

The program task was to design a low-cost wind turbine blade based on a stainless steel - fiberglass-foam Budd blade design concept, to meet NASA Lewis specifications, and to evaluate its principle characteristics, its low cost features, and its advantages and disadvantages. A blade structure was designed and construction methods and materials were selected. A complete blade tooling concepts, various technical and economic analysis, and evaluations of the blade design were performed. A comprehensive fatigue test program was conducted to provide data to verify the design stress allowables. A test specimen of the spar assembly, including the root end attachment was fabricated. This full-scale section, 20 ft. long, will be fatigue tested by NASA.

17. Key Words (Suggested by Author(s))	18. Distribution Statement
Blade design Stainless steel spar Fiberglass surfaces Wind energy conversion system	Unclassified - unlimited STAR Category 44 DOE Category UC-60

19. Security Classif. (of this report)	20. Security Classif. (of this page)	21. No. of Pages	22. Price*
Unclassified	Unclassified		

* For sale by the National Technical Information Service, Springfield, Virginia 22161